

## Antibody-PROTAC Conjugate Enables Selective Degradation of Receptor-Interacting Serine/Threonine-Protein Kinase 2 (RIPK2) in HER+ Cell Lines

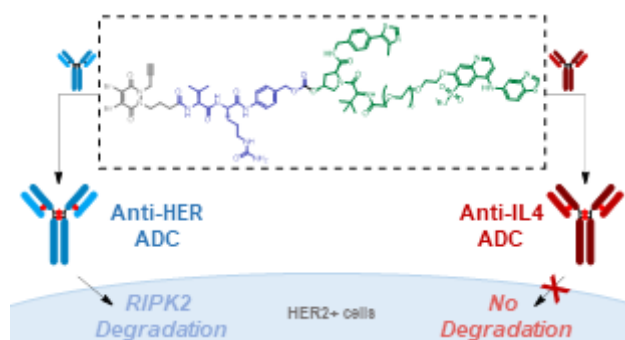
Karina Chan<sup>a,b</sup>, Preethi Soundarya Sathyamurthi<sup>a</sup>, Markus A. Queisser<sup>a</sup>, Michael Mullin<sup>a</sup>, Harry Shrives<sup>a</sup>, Diane M. Coe<sup>a</sup>, Glenn A. Burley<sup>\*b</sup>

<sup>a</sup> GSK, Gunnels Wood Road, Stevenage, Hertfordshire, SG1 2NY, United Kingdom

<sup>b</sup> Department of Pure and Applied Chemistry, University of Strathclyde, Glasgow, G1 1XL, United Kingdom

### ABSTRACT

Proteolysis targeting chimeras (PROTACs) are a family of heterobifunctional molecules that are now realising their promise as a therapeutic strategy for targeted protein degradation. However, one limitation of existing designs is the lack of cell-selective targeting of the protein degrading payload. This manuscript reports a cell-targeted approach to degrade receptor-interacting serine/threonine-protein kinase 2 (RIPK2) in HER2+ cell lines. An antibody-PROTAC conjugate is prepared containing a protease cleavable linkage between the antibody and the corresponding degrader. Potent RIPK2 degradation is observed in HER2+ cell lines, whereas an equivalent anti-IL4 antibody-PROTAC conjugate shows no degradation at therapeutically relevant concentrations. No RIPK2 degradation was observed in HER2- cell lines for both bioconjugates. This work demonstrates the potential for cell-selective delivery of PROTAC scaffolds by engaging with signature extracellular proteins expressed on the surface of particular cell types.



PROTACs are heterobifunctional molecules that selectively degrade a protein of interest (POI).<sup>1,2</sup> The mechanism of action (MoA) of PROTACs proceeds via the formation of a ternary complex with a POI and an E3 ligase, which then induces a proximity-induced ubiquitination of the POI on a surface lysine, and subsequent degradation by the ubiquitin-proteasome pathway.<sup>3,4</sup> A hallmark of these protein degraders is the catalytic nature of degradation,<sup>5</sup> which enables recycling of the PROTAC after dissociation from the ternary complex. This unique MoA results in a longer lasting pharmacological effect relative to conventional non-covalent inhibition,<sup>6</sup> enabling lower dosages for their application *in vivo*.<sup>7-9</sup> A further advantage of PROTACs over conventional inhibitor strategies is the need to engage the POI ultimately for degradation rather than a modulation of protein function by stoichiometric interaction with a small molecule.<sup>10</sup>

At present, one major limitation of the application of PROTACs is their lack of cell selectivity and variable levels of cell permeability,<sup>11</sup> which is reflected in their sub-optimal pharmacokinetic properties.<sup>12,13</sup> Incorporating a cell-targeting module into PROTAC designs has the potential to deliver the PROTAC cargo to the desirable cell type(s), and subsequently, minimise off-target toxicity (Figure 1A). An emerging platform for the cell-selective delivery of PROTACs is their conjugation to an antibody (Ab).<sup>14</sup> Ab-drug conjugates (ADCs) combine the ability to selectively deliver a molecular payload, such as a PROTAC, to specific cell types, thereby bypassing the need for extensive optimization of the cell uptake properties to the PROTAC scaffold (Figure 1B). Whilst Ab-PROTACs have been developed for the cell-selective degradation of BRD4 and ER $\alpha$ ,<sup>15-17</sup> the impact of how the linkage chemistry (*i.e.*, cleavable vs. non-cleavable), drug accumulation into a target cell type and the diversity of POI which can be targeted by Ab conjugation is still in its infancy. Herein, we expand the scope of Ab-PROTAC conjugates by demonstrating the cell-selective and targeted degradation of serine/threonine-protein kinase 2 (RIPK2) in HER+ cell lines (Figure 1C).

We selected a RIPK2 PROTAC **1**<sup>4</sup> and an anti-HER2 monoclonal antibody (mAb), trastuzumab,<sup>18</sup> as our model system to demonstrate selective RIPK2 degradation in HER2+ cells only. Dysregulation of RIPK2-mediated pathways is associated with inflammatory bowel disease,<sup>19</sup> severe pulmonary sarcoidosis,<sup>20</sup> multiple sclerosis,<sup>21</sup> and cancer.<sup>22</sup> We hypothesised that the ability to degrade RIPK2 only in cells which express cancer biomarkers would provide the basis for cell selective targeting.

Our design approach involved covalently linking a RIPK2 PROTAC to each Ab scaffold *via* a disulfide rebridging reagent (dibromopyridazinedione, diBrPD).<sup>23</sup> This approach enabled attachment of the PROTAC linkage to a precise site on the Ab scaffold *i.e.*, at the interchain cysteines.<sup>24</sup> The diBrPD warhead was coupled to the PROTAC *via* a protease cleavable valine-citrulline-*para*-aminobenzyl-alcohol (VC-PAB) linker.<sup>25</sup> A second antibody, anti-IL4 pascalizumab, was also selected as a negative control.<sup>26</sup> A terminal alkyne was incorporated onto the second nitrogen of the diBrPD to act as a flexible handle for potential downstream functionalisation.

The RIPK2 PROTAC **1** was attached to the VC-PAB **S6** *via* a carbonate linkage, which was then linked to the diBrPD by an amide bond (Scheme S3). Conjugation to the anti-HER2 mAb, trastuzumab, was achieved by reduction of the interchain disulfides by TCEP, followed by addition of the diBrPD rebridging reagent **S10** to form conjugate ADC-**2**, which identified a drug-to-Ab ratio (DAR) of 4.0 (Figure 2). These exist as an interchain bridged species, and an intrachain “half body” (HB) species, where the cysteines have bridged within a single heavy chain. The control anti-IL4 ADC-**3** was synthesised in a similar manner, which resulted in a DAR of 3.7.

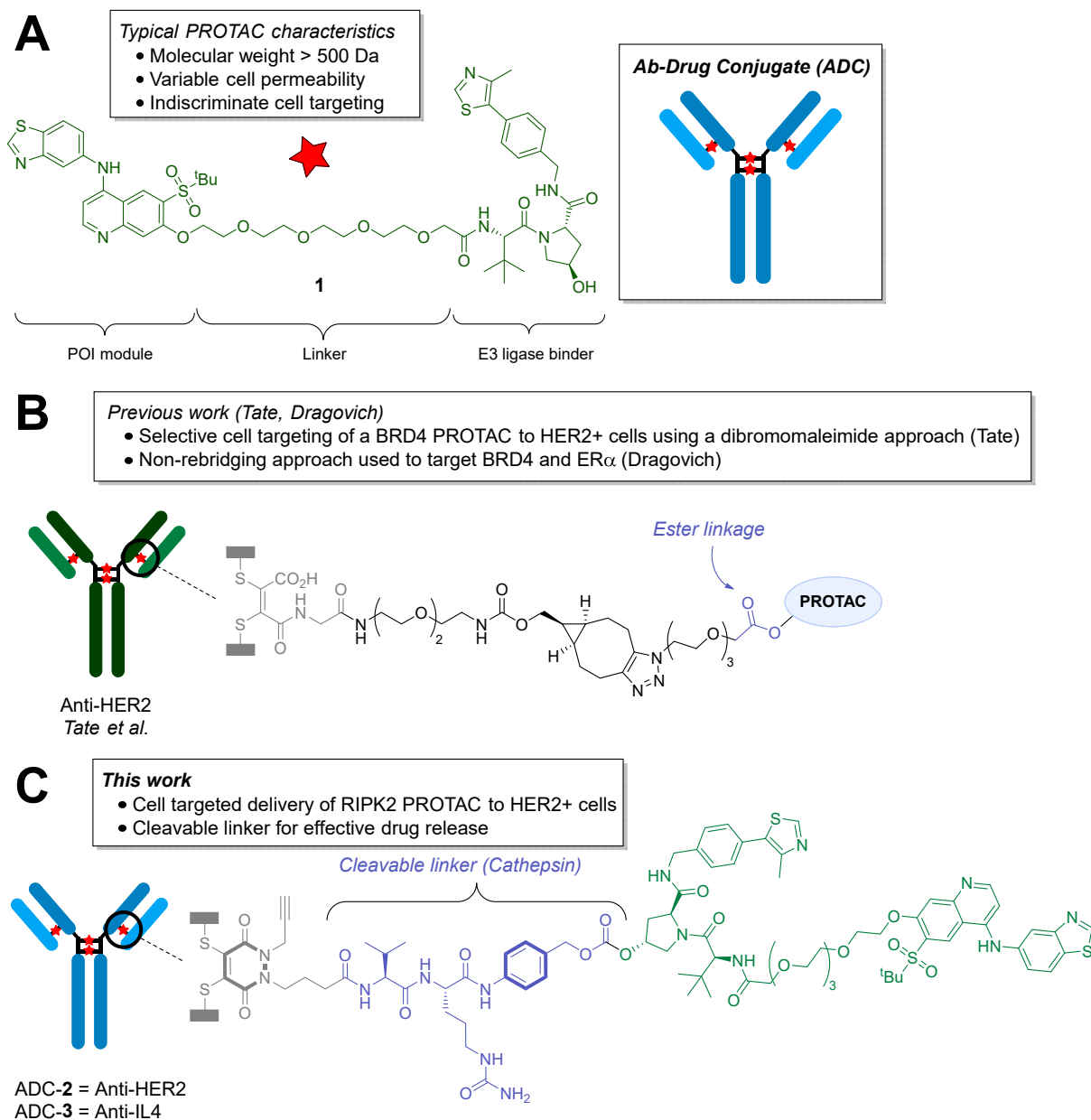


**Figure 1. (A)** General structure and characteristics of a PROTAC and ADCs. **(B)** Exemplar development of Ab-PROTAC conjugates. **(C)** *Our approach*: RIPK2 degrading Ab-PROTAC conjugates incorporating a cleavable linkage. **Gray**: dibromopyridazine-dione (diBrPD) conjugation motif; **Blue**: VC-PAB linker; **Green**: RIPK2 PROTAC.

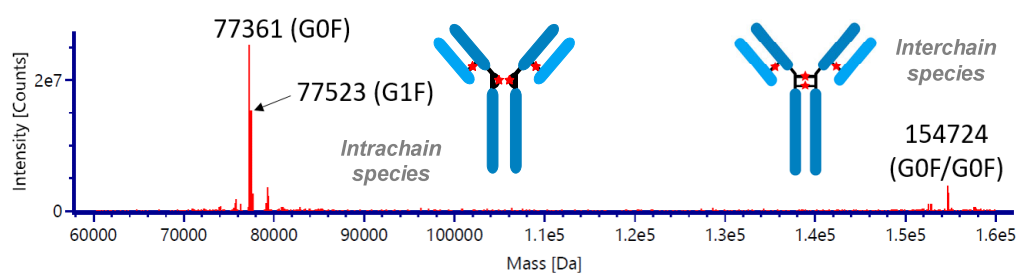


**Figure 2.** Deconvoluted mass spectrum of anti-HER2 ADC-2. Unmodified mAb = 147990 Da. Calculated DAR 4 = 154714 Da, found 154724 (error 10 Da). Calculated half-body (HB) DAR 2 = 77357 Da, found 77361 (error 4 Da). **G0F** and **G1F** correspond to glycan modifications on the mAb.<sup>27</sup>

RIPK2 degradation using ADC-2 and ADC-3 were assessed in a SKOV3 HER2+ breast cancer cell line. The anti-HER2 ADC-2 showed similar levels of RIPK2 degradation compared to the parent PROTAC whereas the anti-IL4 ADC-3 showed no degradation at 10 nM. An unexpected observation was RIPK2 degradation using ADC-3 at concentrations above 100 nM (Figure 3A). As the SKOV3 cells do not have membrane-bound IL-4, we rationalised that the observed degradation might be due to non-specific uptake mechanisms, such as macropinocytosis.<sup>28</sup>

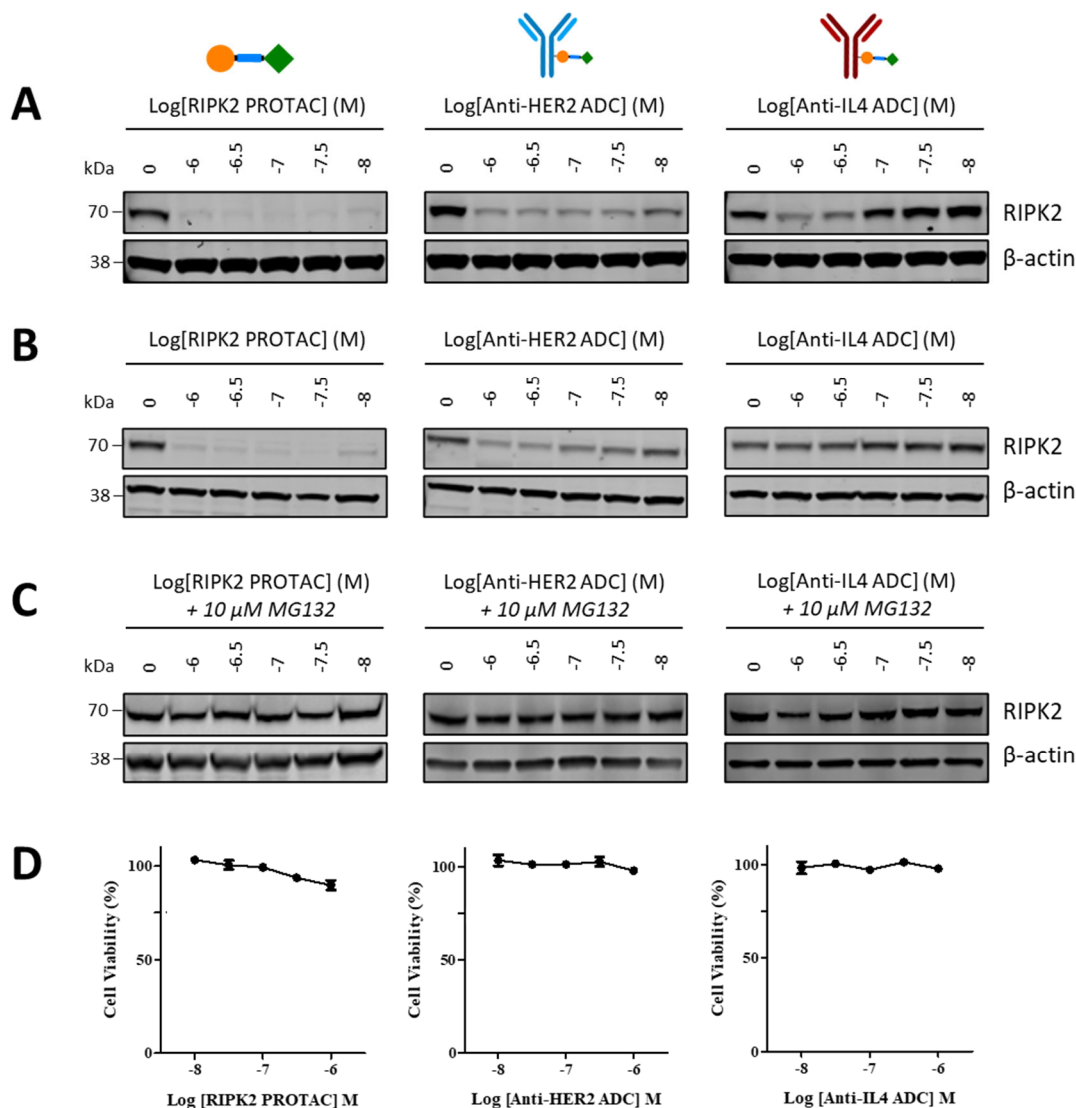


**Figure 3.** RIPK2 degradation of PROTAC 1, ADC-2 and ADC-3 in SKOV3 cells. **(A)** Western blot analysis after 16 h incubation. **(B)** Western blot analysis after 6 h incubation. **(C)** Western blot analysis after a 1 h pre-treatment with 10  $\mu$ M MG132, followed by a 16 h co-treatment with PROTAC 1, ADC-2 or ADC-3. **(D)** CellTiter-Glo<sup>®</sup> cell viability assay carried out in SKOV3 cells following a 16 h incubation with PROTAC 1, ADC-2 or ADC-3.

To rule out instability of the linker causing premature release of PROTAC, ADC-2 was re-analysed after 275 days storage in pH 7.4 PBS at 4  $^{\circ}$ C. Intact MS analysis revealed no degradation of the conjugate, (Figure S1). Shortening of the incubation time (6 h) resulted in less RIPK2 degradation by ADC-2 compared to that of the PROTAC 1 alone (Figure 3B). We surmise that this is due to the uptake and release of the PROTAC from the conjugate slowing down the initial rate of degradation. To confirm RIPK2 degradation was occurring *via* the ubiquitin-proteasome pathway, SKOV3 cells were treated with PROTAC 1, ADC-2 or ADC-3 in the presence of 10  $\mu$ M MG132, a known proteasome inhibitor.<sup>29</sup>

No degradation was observed for all compounds, confirming that degradation is *via* a proteasome dependent pathway (Figure 3C). No cytotoxicity was observed up to 1  $\mu$ M for both ADC-1 and ADC-2 (Figure 3D).

Cell-selective targeting of ADC-2 and ADC-3 was then tested in a HEK293 HER2- cell line using a HiBIT assay. Both ADC-2 and ADC-3 exhibited RIPK2 degradation at higher concentrations, with a more prominent effect as the concentration exceeded 100 nM. This agrees with the similar degradation observed in SKOV3 cells is likely due to non-specific uptake. Most importantly, no degradation was observed at 10 nM for both conjugates compared to 50% degradation when PROTAC 1 was used (Figure 4A). Again, no cytotoxicity was observed for all compounds (Figure 4B).

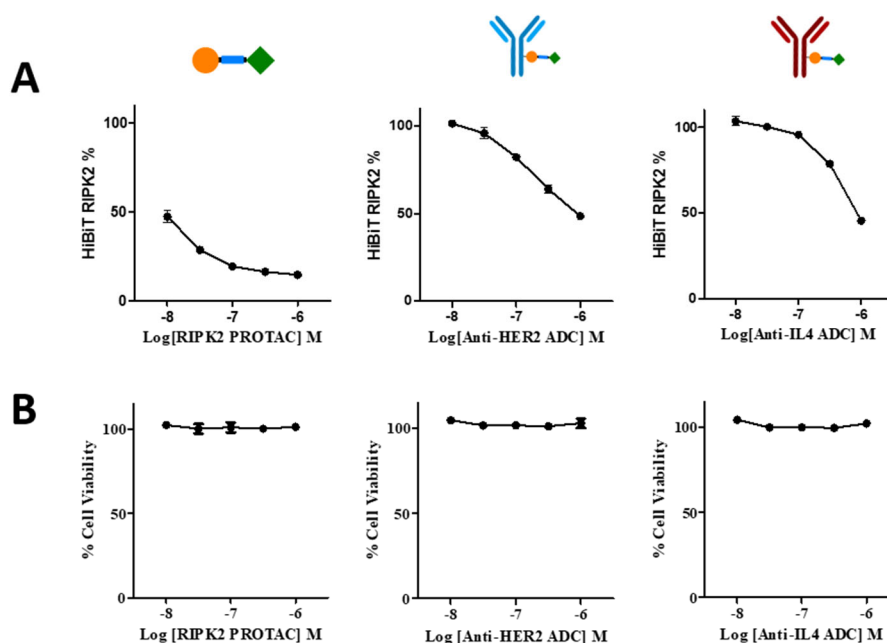


**Figure 4. (A)** RIPK2 levels in a RIPK2 HiBIT HEK293 cell line after a 16 h incubation with PROTAC 1, ADC-2 or ADC-3. RIPK2 levels determined using the Promega Nano-Glo HiBIT Lytic Detection system. **(B)** CellTiter-Glo<sup>®</sup> cell viability assay carried out in HEK293 cells following a 16 h incubation with PROTAC 1, ADC-2 or ADC-3.

In summary, we have demonstrated cell-selective degradation of RIPK2 in HER2+ and SKOV3 cells using an Ab-PROTAC conjugate. This approach complements ADC developments and provides a design strategy to use PROTACs which have sub-optimal physicochemical properties or where cell selective delivery of the PROTAC payload is required.

## EXPERIMENTAL

A description of all methods, assays and experimental procedures for the synthesis of all compounds are available in the Supporting Information.

## ACKNOWLEDGEMENTS

The authors thank GSK and the University of Strathclyde collaborative PhD program in Synthetic Organic and Medicinal Chemistry for funding and scientific resources, as well as the EPSRC for funding via Prosperity Partnership EP/S035990/1.

## REFERENCES

- (1) Békés, M.; Langley, D. R.; Crews, C. M. PROTAC targeted protein degraders: the past is prologue. *Nat. Rev. Drug Discov.* **2022**, *21*, 181-200.
- (2) Diehl, C. J.; Ciulli, A. Discovery of small molecule ligands for the von Hippel-Lindau (VHL) E3 ligase and their use as inhibitors and PROTAC degraders. *Chem. Soc. Rev.* **2022**, *51*, 8216-8257.

- (3) Sakamoto, K. M.; Kim, K. B.; Kumagai, A.; Mercurio, F.; Crews, C. M.; Deshaies, R. J. Protacs: Chimeric molecules that target proteins to the Skp1-Cullin-F box complex for ubiquitination and degradation. *Proc. Natl. Acad. Sci. U. S. A.* **2001**, *98*, 8554-8559.
- (4) Bondeson, D. P.; Mares, A.; Smith, I. E. D.; Ko, E.; Campos, S.; Miah, A. H.; Mulholland, K. E.; Routly, N.; Buckley, D. L.; Gustafson, J. L.; et al. Catalytic in vivo protein knockdown by small-molecule PROTACs. *Nat. Chem. Biol.* **2015**, *11*, 611-617.
- (5) Yan, J. Y.; Li, T. F.; Miao, Z. Y.; Wang, P.; Sheng, C. Q.; Zhuang, C. L. Homobivalent, Trivalent, and Covalent PROTACs: Emerging Strategies for Protein Degradation. *J. Med. Chem.* **2013**, *56*, 8798-8827.
- (6) Nemeč, V.; Schwalm, M. P.; Müller, S.; Knapp, S. PROTAC degraders as chemical probes for studying target biology and target validation. *Chem. Soc. Rev.* **2022**, *51*, 7971-7993.
- (7) Burslem, G. M.; Smith, B. E.; Lai, A. C.; Jaime-Figueroa, S.; McQuaid, D. C.; Bondeson, D. P.; Toure, M.; Dong, H. Q.; Qian, Y. M.; Wang, J.; et al. The Advantages of Targeted Protein Degradation Over Inhibition: An RTK Case Study. *Cell Chem. Biol.* **2018**, *25*, 67-77.
- (8) Tinworth, C. P.; Lithgow, H.; Dittus, L.; Bassi, Z. I.; Hughes, S. E.; Muelbaier, M.; Dai, H.; Smith, I. E. D.; Kerr, W. J.; Burley, G. A.; et al. PROTAC-Mediated Degradation of Bruton's Tyrosine Kinase Is Inhibited by Covalent Binding. *ACS Chem. Biol.* **2019**, *14*, 342-347.
- (9) Schneider, M.; Radoux, C. J.; Hercules, A.; Ochoa, D.; Dunham, I.; Zalmas, L.-P.; Hessler, G.; Ruf, S.; Shanmugasundaram, V.; Hann, M. M.; et al. The PROTACtable genome. *Nat. Rev. Drug Discov.* **2021**, *20*, 789-797.
- (10) Shimokawa, K.; Shibata, N.; Sameshima, T.; Miyamoto, N.; Ujikawa, O.; Nara, H.; Ohoka, N.; Hattori, T.; Cho, N.; Naito, M. Targeting the Allosteric Site of Oncoprotein BCR-ABL as an Alternative Strategy for Effective Target Protein Degradation. *ACS Med. Chem. Lett.* **2017**, *8*, 1042-1047.
- (11) Yokoo, H.; Naito, M.; Demizu, Y. Investigating the cell permeability of proteolysis-targeting chimeras (PROTACs). *Expert. Opin. Drug Discov.* **2023**, *18*, 357-361.
- (12) Benowitz, A. B.; Scott-Stevens, P. T.; Harling, J. D. Challenges and opportunities for in vivo PROTAC delivery. *Future Med. Chem.* **2022**, *14*, 119-121.
- (13) Guenette, R. G.; Yang, S. W.; Min, J.; Pei, B.; Potts, P. R. Target and tissue selectivity of PROTAC degraders. *Chem. Soc. Rev.* **2022**, *51*, 5740-5756.
- (14) Dragovich, P. S. Degradation-antibody conjugates. *Chem. Soc. Rev.* **2022**, *51*, 3886-3897.
- (15) Dragovich, P. S.; Pillow, T. H.; Blake, R. A.; Sadowsky, J. D.; Adaligil, E.; Adhikari, P.; Chen, J. H.; Corr, N.; Dela Cruz-Chuh, J.; Del Rosario, G.; et al. Antibody-Mediated Delivery of Chimeric BRD4 Degradation. Part 2: Improvement of In Vitro Antiproliferation Activity and In Vivo Antitumor Efficacy. *J. Med. Chem.* **2021**, *64*, 2576-2607.
- (16) Dragovich, P. S.; Adhikari, P.; Blake, R. A.; Blaquiere, N.; Chen, J. H.; Cheng, Y. X.; den Besten, W.; Han, J. P.; Hartman, S. J.; He, J. T.; et al. Antibody-mediated delivery of chimeric protein degraders which target estrogen receptor alpha (ER alpha). *Bioorg. Med. Chem. Lett.* **2020**, *30*, 126907.
- (17) Maneiro, M. a.; Forte, N.; Shchepinova, M. M.; Kounde, C. S.; Chudasama, V.; Baker, J. R.; Tate, E. W. Antibody-PROTAC Conjugates Enable HER2-Dependent Targeted Protein Degradation of BRD4. *ACS Chem. Biol.* **2020**, *15*, 1306-1312.
- (18) Claret, F.; Vu, T. Trastuzumab: Updated Mechanisms of Action and Resistance in Breast Cancer. *Front. Oncol.* **2012**, *2*, 62.
- (19) Biswas, A.; Liu, Y.-J.; Hao, L.; Mizoguchi, A.; Salzman, N. H.; Bevins, C. L.; Kobayashi, K. S. Induction and rescue of Nod2-dependent Th1-driven granulomatous inflammation of the ileum. *Proc. Natl. Acad. Sci. U. S. A.* **2010**, *107*, 14739-14744.
- (20) Sato, H.; Williams, H. R. T.; Spagnolo, P.; Abdallah, A.; Ahmad, T.; Orchard, T. R.; Copley, S. J.; Desai, S. R.; Wells, A. U.; Bois, R. M. d.; et al. CARD15/NOD2 polymorphisms are associated with severe pulmonary sarcoidosis. *Eur. Respir. J.* **2010**, *35*, 324-330.
- (21) Shaw, P. J.; Barr, M. J.; Lukens, J. R.; McGargill, M. A.; Chi, H.; Mak, T. W.; Kanneganti, T.-D. Signaling via the RIP2 Adaptor Protein in Central Nervous System-Infiltrating Dendritic Cells Promotes Inflammation and Autoimmunity. *Immunity* **2011**, *34*, 75-84.

- (22) Haile, P. A.; Votta, B. J.; Marquis, R. W.; Bury, M. J.; Mehlmann, J. F.; Singhaus, R., Jr.; Charnley, A. K.; Lakdawala, A. S.; Convery, M. A.; Lipshutz, D. B.; et al. The Identification and Pharmacological Characterization of 6-(tert-Butylsulfonyl)-N-(5-fluoro-1H-indazol-3-yl)quinolin-4-amine (GSK583), a Highly Potent and Selective Inhibitor of RIP2 Kinase. *J. Med. Chem.* **2016**, *59*, 4867-4880.
- (23) Maruani, A.; Smith, M. E. B.; Miranda, E.; Chester, K. A.; Chudasama, V.; Caddick, S. A plug-and-play approach to antibody-based therapeutics via a chemoselective dual click strategy. *Nat. Commun.* **2015**, *6*, 6645
- (24) Chudasama, V.; Maruani, A.; Caddick, S. Recent advances in the construction of antibody–drug conjugates. *Nat. Chem.* **2016**, *8*, 114-119.
- (25) Dubowchik, G. M.; Firestone, R. A.; Padilla, L.; Willner, D.; Hofstead, S. J.; Mosure, K.; Knipe, J. O.; Lasch, S. J.; Trail, P. A. Cathepsin B-Labile Dipeptide Linkers for Lysosomal Release of Doxorubicin from Internalizing Immunoconjugates: Model Studies of Enzymatic Drug Release and Antigen-Specific In Vitro Anticancer Activity. *Bioconjugate Chem.* **2002**, *13*, 855-869.
- (26) HART, T. K.; BLACKBURN, M. N.; BRIGHAM-BURKE, M.; DEDE, K.; AL-MAHDI, N.; ZIA-AMIRHOSSEINI, P.; COOK, R. M. Preclinical efficacy and safety of pascolizumab (SB 240683): a humanized anti-interleukin-4 antibody with therapeutic potential in asthma. *Clin. Exp. Immunol.* **2002**, *130*, 93-100.
- (27) Yang, X.; Bartlett, M. G. Glycan analysis for protein therapeutics. *J. Chromatogr. B* **2019**, *1120*, 29-40.
- (28) Commisso, C. The pervasiveness of macropinocytosis in oncological malignancies. *Philos. Trans. R. Soc. Lond. B* **2019**, *374*, 20180153.
- (29) Lu, J.; Qian, Y. M.; Altieri, M.; Dong, H. Q.; Wang, J.; Raina, K.; Hines, J.; Winkler, J. D.; Crew, A. P.; Coleman, K.; et al. Hijacking the E3 Ubiquitin Ligase Cereblon to Efficiently Target BRD4. *Chem. Biol.* **2015**, *22*, 755-763.

Supporting information for:

# Antibody-PROTAC Conjugate Enables Selective Degradation of Receptor-Interacting Serine/Threonine-Protein Kinase 2 (RIPK2) in HER+ Cell Lines

Karina Chan<sup>a,b</sup>, Preethi Soundarya Sathyamurthi<sup>a</sup>, Markus A. Queisser<sup>a</sup>, Michael Mullin<sup>a</sup>, Harry Shrivess<sup>a</sup>, Diane M. Coe<sup>a</sup>, Glenn A. Burley<sup>\*b</sup>

<sup>a</sup>GSK, Gunnels Wood Road, Stevenage, Hertfordshire, SG1 2NY, United Kingdom

<sup>b</sup>Department of Pure and Applied Chemistry, University of Strathclyde, Glasgow, G1 1XL, United Kingdom

## Table of Contents

<b>1. Chemistry</b> .....	<b>2</b>
<b>1.1</b> General experimental procedures .....	2
<b>1.2</b> RIPK2 PROTAC <b>1</b> .....	4
<b>1.3</b> Dibromopyridazinedione <b>S3</b> .....	5
<b>1.4</b> Boc-Val-Cit-PAB linker <b>S6</b> .....	8
<b>1.5</b> Conjugation reagent: diBrPD-VC-PABC-PROTAC <b>S10</b> .....	11
<b>1.6</b> NMR Spectra .....	16
<b>2. Biology and Bioconjugation</b> .....	<b>24</b>
<b>2.1</b> Materials and methods .....	24
<b>2.2</b> Expression of mAbs .....	25
<b>2.3</b> Synthesis of ADC- <b>2</b> and ADC- <b>3</b> .....	25
<b>2.4</b> Mass Spectrometry of ADC- <b>2</b> and ADC- <b>3</b> .....	26
<b>2.5</b> SDS-PAGE of ADC- <b>2</b> and ADC- <b>3</b> .....	28
<b>3. Biological Assays</b> .....	<b>29</b>
<b>3.1</b> Materials and Methods.....	29
<b>3.2</b> Uncropped blots .....	30
<b>4. References</b> .....	<b>33</b>

# 1. Chemistry

## 1.1 General experimental procedures

### Solvents and reagents

Solvents and reagents were purchased from commercial suppliers and used as received. Reactions were monitored by liquid chromatography-mass spectroscopy (LCMS) or thin-layer chromatography (TLC). Prior to commencing all reactions, reaction vessels were sealed, evacuated, and backfilled with  $N_{2(g)}$  ( $\times 3$ ) to ensure the presence of an inert atmosphere.

### Thin-layer chromatography (TLC)

TLC was carried out using polyester-backed pre-coated silica plates (0.2 mm particle size). Spots were visualised under ultraviolet light of  $\lambda_{max} = 254$  nm. In cases where spots were difficult to visualise, the plate was stained with  $KMnO_4$  (potassium permanganate) or ninhydrin before gentle heating.

### Flash column chromatography

Column chromatography was carried out using the Teledyne ISCO CombiFlash® Rf+ apparatus with RediSep® silica cartridges (normal-phase), Biotage® SNAP KP-C18 cartridges (reverse-phase) or an EZ Prep® column (preparatory HPLC). Eluent conditions are stated in a form describing a gradient of the minor solvent (e.g. EtOAc) in the major solvent (e.g. cyclohexane).

### Liquid chromatography mass spectrometry (LCMS)

LCMS analysis was completed on a Waters® Acquity UPLC instrument equipped with a BEH (ethylene-bridged hybrid) column (50 mm  $\times$  2.1 mm with 1.7  $\mu$ m packing diameter) and a Waters® Micromass ZQ MS using alternate-scan positive and negative electrospray ionisation. Analytes were detected as a summed UV wavelength spectra between 210-350 nm. Mass to charge (m/z) ratios are shown in Daltons. Two LCMS methods were used:

- **Formic:** 40 °C, 1 mL/min flow rate, using a mobile phase gradient of water containing 0.1% formic acid (v/v) and acetonitrile containing 0.1% formic acid (v/v). Gradient conditions were initially 1% of the acetonitrile mixture, increasing linearly to 97% over 1.5 min, before remaining at 97% for 0.4 min, then rising to 100% over 0.1 min.
- **High pH:** 40 °C, 1 mL/min flow rate, using a mobile phase gradient of water containing aq. ammonium bicarbonate (10 mM, adjusted to pH 10 with 0.88 M aqueous ammonia) and acetonitrile. Gradient conditions were initially 1% of the acetonitrile mixture, increasing linearly to 97% over 1.5 min, before remaining at 97% for 0.4 min, then rising to 100% over 0.1 min.

### High-resolution mass spectrometry (HRMS)

HRMS analysis were conducted on a Waters XEVO G2-XS quadrupole time-of-flight (QToF) mass spectrometer instrument. Mass to charge ( $m/z$ ) ratios are shown in Daltons. LCMS analysis has been carried out using one of the following methods:

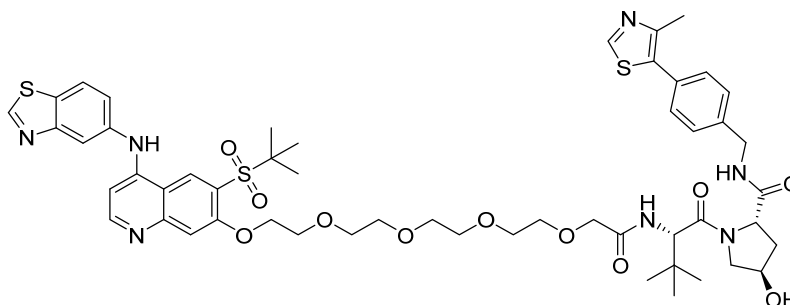
- **10 min Formic:** Ionisation mode: Positive Electrospray. Acquity UPLC CSH C18 column (100 mm x 2.1 mm, 1.7  $\mu\text{m}$  packing diameter) at 50 °C, 0.8 mL/min flow rate. Gradient elution with the eluents as water containing 0.1% volume/volume (v/v) formic acid and (B) MeCN. The UV detection was a summed signal from wavelength of 210 nm to 350 nm. Injection volume: 0.2  $\mu\text{L}$ . The elution conditions began with 5% MeCN mixture, increasing to 93% over 6 minutes, before remaining at 93% for 0.5 minutes, decreasing back to 5% MeCN mixture for 0.5 minutes before equilibrating for 0.5 minutes.
- **20 min High pH:** Ionisation mode: Positive Electrospray. Acquity UPLC BEH C18 column (100 mm x 2.1 mm, 1.7  $\mu\text{m}$  packing diameter) at 50 °C, 0.8 mL/min flow rate. Gradient elution with the eluents as 10 mM ammonium bicarbonate in water adjusted to pH 10 with ammonia solution and MeCN. The UV detection was a summed signal from wavelength of 210 nm to 500 nm. Injection volume: 0.2  $\mu\text{L}$ . The elution conditions began with 1% MeCN mixture, increasing to 90% over 17 minutes, before remaining at 90% for 1.5 minutes, decreasing back to 1% MeCN mixture for 1.0 minutes before equilibrating for 1.0 minutes.

### Nuclear magnetic resonance spectroscopy (NMR)

Proton ( $^1\text{H}$ ) and carbon ( $^{13}\text{C}$ ) spectra were measured on a Bruker AV400 ( $^1\text{H}$  = 400 MHz,  $^{13}\text{C}$  = 101 MHz) spectrometer. Chemical shifts are reported in ppm, relative to the chemical shift of tetramethylsilane (TMS = 0.00 ppm) or the following solvent peaks:  $\text{CDCl}_3$  ( $^1\text{H}$  = 7.26 ppm,  $^{13}\text{C}$  = 77.2 ppm),  $\text{CD}_3\text{OD}$  ( $^1\text{H}$  = 3.31 ppm,  $^{13}\text{C}$  = 49.0 ppm), or  $(\text{CD}_3)_2\text{SO}$  ( $^1\text{H}$  = 2.50 ppm,  $^{13}\text{C}$  = 39.5 ppm). Peak assignments are stated as chemical shifts, integrations, and coupling constants (where relevant). Coupling constants are quoted to the nearest 0.1 Hz and multiplicities described as either singlet (s), doublet (d), triplet (t), quartet (q), quintet (quin), sextet (sxt), septet (sept), broad (br), or multiplet (m).

## 1.2 RIPK2 PROTAC 1

(2*S*,4*R*)-1-((*S*)-17-((4-(Benzo[*d*]thiazol-5-ylamino)-6-(*tert*-butylsulfonyl)quinolin-7-yl)oxy)-2-(*tert*-butyl)-4-oxo-6,9,12,15-tetraoxa-3-azaheptadecanoyl)-4-hydroxy-*N*-(4-(4-methylthiazol-5-yl)benzyl)pyrrolidine-2-carboxamide (**1**)

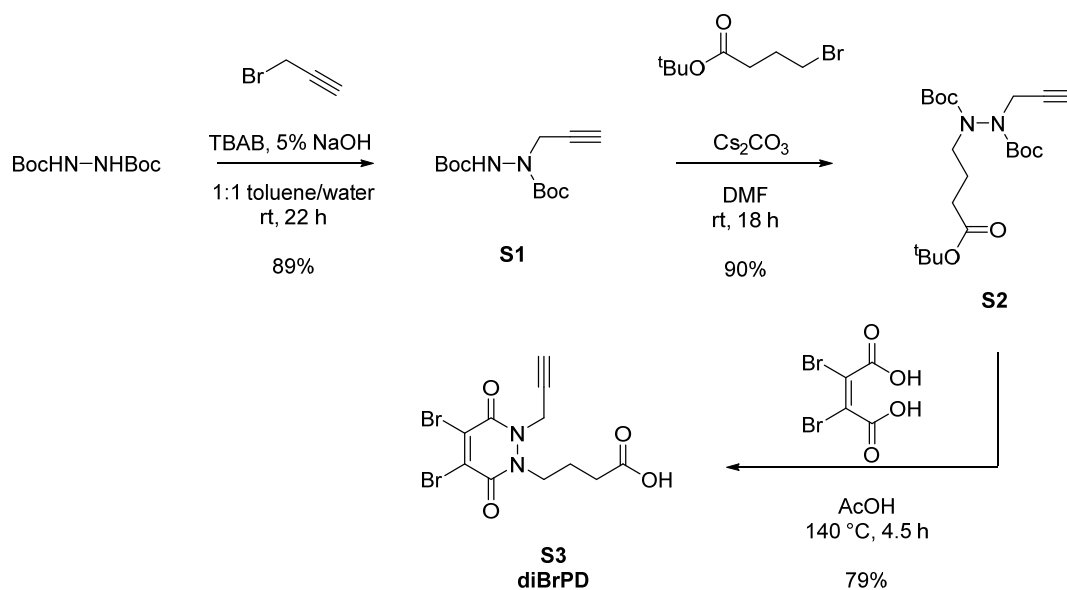


$^1\text{H NMR}$  (400 MHz,  $\text{DMSO-}d_6$ ):  $\delta$  9.50 - 9.41 (m, 1H), 9.02 (s, 1H), 8.99 - 8.93 (m, 1H), 8.58 (br t,  $J = 6.1$  Hz, 1H), 8.48 (d,  $J = 5.8$  Hz, 1H), 8.24 (d,  $J = 8.7$  Hz, 1H), 8.07 (d,  $J = 2.1$  Hz, 1H), 7.55 (dd,  $J = 2.1, 8.7$  Hz, 1H), 7.48 (s, 1H), 7.44 - 7.35 (m, 5H), 6.87 (d,  $J = 5.8$  Hz, 1H), 5.14 (br s, 1H), 4.57 (d,  $J = 9.5$  Hz, 1H), 4.49 - 4.31 (m, 3H), 4.30 - 4.22 (m, 1H), 3.97 (s, 2H), 3.87 - 3.81 (m, 2H), 3.72 - 3.48 (m, 16H), 2.44 (s, 3H), 2.11 - 2.03 (m, 1H), 1.96 - 1.87 (m, 1H), 1.40 - 1.30 (m, 9H), 1.00 - 0.90 (m, 9H). Aniline NH not observed.

**LCMS** (High pH):  $t_R = 1.08$  min,  $([\text{M}+\text{H}]^+ 1060.1$ , (99% purity).

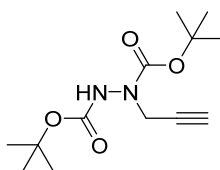
The synthesis of **S1** was carried out as reported in *Nat. Chem. Biol.* **2015**, *11*, 611-617.<sup>1</sup>

### 1.3 Dibromopyridazinedione **S3**



**Scheme S1.** Synthesis of diBrPD **S3**.

#### Di-tert-butyl 1-(prop-2-yn-1-yl)hydrazine-1,2-dicarboxylate (**S1**)



To a suspension of di-tert-butyl hydrazine-1,2-dicarboxylate (3 g, 12.9 mmol) in toluene (20 mL) was added tetrabutylammonium bromide (0.125 g, 0.39 mmol), 3-bromoprop-1-yne (4.32 mL, 38.7 mmol) and 5% aqueous NaOH (20 mL) and the resulting biphasic mixture stirred at rt for 18 h. The mixture was diluted with water (150 mL) and extracted with ethyl acetate (3 × 80 mL). The combined organics were washed with brine (150 mL), passed through a hydrophobic frit and concentrated *in vacuo*. The residue was dried under vacuum to afford **S1** as an orange solid (3.49 g, 12.9 mmol, 100% yield).

**<sup>1</sup>H NMR** (400 MHz, CDCl<sub>3</sub>): δ 6.51 (br s, 1H), 4.28 (br s, 2H), 2.25 (t, *J* = 2.6 Hz, 1H), 1.57 - 1.43 (m, 18H) (Major rotamer reported).

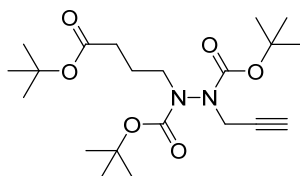
**<sup>13</sup>C NMR** (101 MHz, CDCl<sub>3</sub>): δ 154.6, 81.9, 81.5, 78.7, 72.0, 39.4, 28.2.

**IR**  $\nu_{\text{max}}$  (neat): 3310, 3291, 2980, 2937, 1728, 1689, 1513 cm<sup>-1</sup>.

**m.p.:** 98-100 °C.

**TLC** (1:1 EtOAc/cyclohexane, visualisation = KMnO<sub>4</sub>): R<sub>f</sub> = 0.52.

### Di-tert-butyl 1-(4-(tert-butoxy)-4-oxobutyl)-2-(prop-2-yn-1-yl)hydrazine-1,2-dicarboxylate (**S2**)



To a stirred solution of **S1** (3.4 g, 12.6 mmol) in DMF (50 mL) was added Cs<sub>2</sub>CO<sub>3</sub> (6.15 g, 18.9 mmol) and tert-butyl 4-bromobutanoate (2.5 mL, 13.2 mmol). The resulting mixture was stirred at rt for 17 h. The mixture was diluted with water (200 mL) and extracted with ethyl acetate (3 × 80 mL). The combined organics were washed with 5% aqueous LiCl (3 × 50 mL), passed through a hydrophobic frit and concentrated *in vacuo*. The oil was purified by flash column chromatography, eluting 0-15% EtOAc in cyclohexane on a 80 g silica column over 20 CV. Fractions containing product were combined and concentrated *in vacuo* to afford **S2** as a light yellow oil (4.99 g, 12.1 mmol, 96% yield).

<sup>1</sup>H NMR (400 MHz, CDCl<sub>3</sub>): δ 4.69 - 4.28 (m, 1H), 4.25 - 3.92 (m, 1H), 3.68 - 3.30 (m, 2H), 2.38 - 2.18 (m, 3H), 2.04 - 1.85 (m, 2H), 1.74 - 1.24 (m, 27H). Rotamers observed.

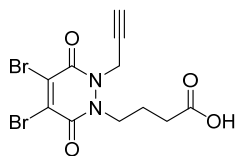
<sup>13</sup>C NMR (101 MHz, CDCl<sub>3</sub>): δ 172.4, 154.6, 154.4, 81.8, 81.1, 80.1, 78.4, 72.8, 49.3, 39.3, 33.2, 28.24, 28.19, 28.1, 23.4. Rotamers observed.

HRMS (ESI): calculated for C<sub>21</sub>H<sub>36</sub>N<sub>2</sub>O<sub>6</sub>Na (*m/z*) [M+Na]<sup>+</sup> requires 435.2471, found [M+Na]<sup>+</sup> 435.2471 (error 0.0 ppm).

IR ν<sub>max</sub> (neat): 3262, 2977, 2933, 1709, 1478, 1456 cm<sup>-1</sup>.

TLC (3:7 EtOAc/Cyclohexane, visualisation = KMnO<sub>4</sub>): R<sub>f</sub> = 0.46.

### 4-(4,5-Dibromo-3,6-dioxo-2-(prop-2-yn-1-yl)-3,6-dihydropyridazin-1(2H)-yl)butanoic acid (**S3**)



A solution of 2,3-dibromomaleic acid (1 g, 3.65 mmol) in AcOH (25 mL) was heated to reflux and left to stir for 30 min prior to addition of **S2** (1.3 g, 3.15 mmol) in AcOH (5 mL). The solution turned from colourless to brown. The reaction mixture was heated to reflux for an additional 4 h before concentration *in vacuo* to give a brown oil. The crude product was purified by flash column

chromatography, eluting 25-60% EtOAc [1% AcOH] in cyclohexane on a 120 g silica column over 20 CV. Fractions containing product were combined and concentrated *in vacuo* to afford **S3** as a pale yellow solid (985 mg, 2.5 mmol, 79% yield).

**<sup>1</sup>H NMR** (400 MHz, CD<sub>3</sub>OD): δ 5.06 (d, *J* = 2.4 Hz, 2H), 4.34 - 4.25 (m, 2H), 2.95 (t, *J* = 2.4 Hz, 1H), 2.44 (t, *J* = 6.8 Hz, 2H), 2.07 - 1.97 (m, 2H). OH not observed.

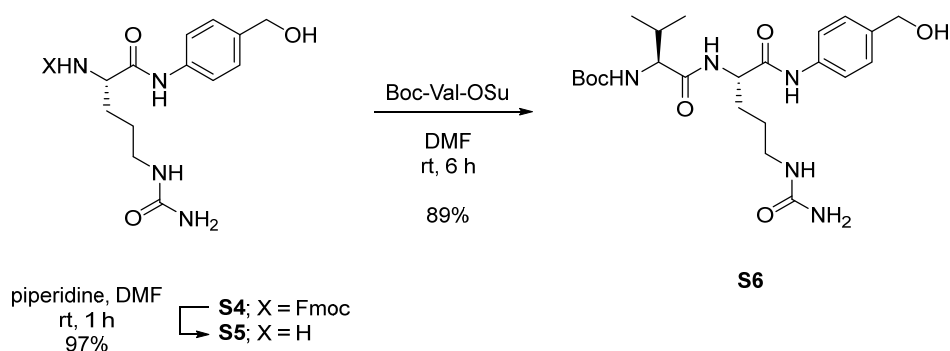
**<sup>13</sup>C NMR** (101 MHz, CD<sub>3</sub>OD): δ 174.7, 153.6, 153.2, 136.1, 134.9, 75.8, 74.5, 46.9, 36.8, 29.9, 22.5.

**LCMS** (Formic): *t<sub>R</sub>* = 0.72 min, [M(Br<sup>79</sup>Br<sup>79</sup>)+H]<sup>+</sup> 393.1, [M(Br<sup>79</sup>Br<sup>81</sup>)+H]<sup>+</sup> 395.0, [M(Br<sup>81</sup>Br<sup>81</sup>)+H]<sup>+</sup> 397.0, (100% purity).

**HRMS** (ESI): calculated for C<sub>11</sub>H<sub>11</sub>Br<sub>2</sub>N<sub>2</sub>O<sub>4</sub> (*m/z*) [M+H]<sup>+</sup> requires 392.9086, found [M+H]<sup>+</sup> 392.9085 (error -0.3 ppm).

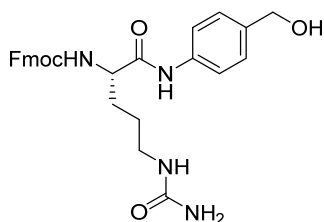
**IR** *v*<sub>max</sub> (neat): 3287, 2938, 2131, 1693, 1639, 1575 cm<sup>-1</sup>.

## 1.4 Boc-Val-Cit-PAB linker **S6**



**Scheme S2.** Synthesis of Boc-VC-PAB linker **S6**.

### (9H-Fluoren-9-yl)methyl (S)-1-((4-(hydroxymethyl)phenyl)amino)-1-oxo-5-ureidopentan-2-yl)carbamate (**S4**)

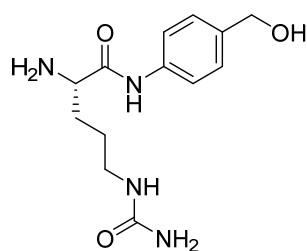


$^1\text{H NMR}$  (400 MHz,  $\text{DMSO}-d_6$ ):  $\delta$  10.08 - 9.91 (m, 1H), 7.90 (d,  $J = 7.6$  Hz, 2H), 7.80 - 7.71 (m, 2H), 7.64 (d,  $J = 8.1$  Hz, 1H), 7.57 (d,  $J = 8.6$  Hz, 2H), 7.46 - 7.39 (m, 2H), 7.38 - 7.30 (m, 2H), 7.25 (d,  $J = 8.6$  Hz, 2H), 5.98 (br t,  $J = 5.6$  Hz, 1H), 5.41 (s, 2H), 5.08 (t,  $J = 5.6$  Hz, 1H), 4.44 (d,  $J = 5.6$  Hz, 2H), 4.33 - 4.12 (m, 4H), 3.12 - 2.90 (m, 2H), 1.76 - 1.56 (m, 2H), 1.55 - 1.34 (m, 2H).

**LCMS** (High pH):  $t_R = 0.96$  min,  $[\text{M}+\text{H}]^+ 503.1$ , (98% purity).

The synthesis of **S4** was carried out as reported in *Angew. Chem., Int. Ed. Engl.* **2021**, *60*, 21691-21696.<sup>2</sup>

### (S)-2-Amino-N-(4-(hydroxymethyl)phenyl)-5-ureidopentanamide (S5)



To a solution of **S4** (6.22 g, 12.4 mmol) in DMF (20 mL) was added piperidine (2.45 mL, 24.8 mmol), and the resulting solution stirred at rt for 1 h. The reaction mixture was diluted with water (100 mL) and filtered under vacuum, washing the solid with additional water (100 mL). The filtrate was washed with diethyl ether (50 mL), then EtOAc (50 mL), and the aqueous layer was then concentrated *in vacuo* to afford **S5** as a white solid (3.45 g, 11.9 mmol, 97% yield).

<sup>1</sup>H NMR (400 MHz, DMSO-*d*<sub>6</sub>): δ 10.37 - 9.42 (m, 1H), 7.58 (d, *J* = 8.6 Hz, 2H), 7.24 (d, *J* = 8.6 Hz, 2H), 5.94 (br t, *J* = 5.6 Hz, 1H), 5.35 (s, 2H), 5.17 - 4.97 (m, 1H), 4.44 (s, 2H), 3.31 - 3.27 (m, 1H), 3.05 - 2.91 (m, 2H), 1.70 - 1.56 (m, 1H), 1.55 - 1.34 (m, 3H). NH<sub>2</sub> protons not observed.

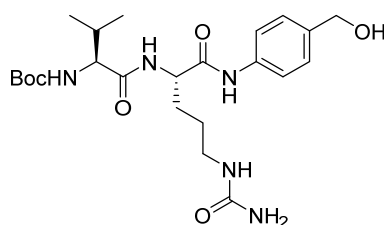
<sup>13</sup>C NMR (101 MHz, DMSO-*d*<sub>6</sub>): δ 174.8, 159.2, 138.0, 137.7, 127.4, 119.3, 63.1, 55.7, 33.1, 27.2.

LCMS (High pH): *t*<sub>R</sub> = 0.40 min, [M+H]<sup>+</sup> 281.3, (100% purity).

HRMS (ESI): calculated for C<sub>13</sub>H<sub>21</sub>N<sub>4</sub>O<sub>3</sub> (*m/z*) [M+H]<sup>+</sup> requires 281.1614, found [M+H]<sup>+</sup> 281.1602 (error -4.3 ppm).

IR *v*<sub>max</sub> (neat): 3304, 2929, 2865, 1654, 1605, 1541 cm<sup>-1</sup>.

### *Tert*-butyl ((S)-1-(((S)-1-((4-(hydroxymethyl)phenyl)amino)-1-oxo-5-ureidopentan-2-yl)amino)-3-methyl-1-oxobutan-2-yl)carbamate (S6)



**S5** (260 mg, 0.93 mmol) and Boc-Val-OSu (292 mg, 0.93 mmol) were combined in DMF (1 mL) and the resulting mixture stirred at rt for 6 h. The reaction mixture was purified directly by reverse phase chromatography, eluting 15-55% acetonitrile in water with a 10 mM ammonium bicarbonate modifier

adjusted to pH 10. Fractions containing product were combined and concentrated *in vacuo* to afford **S6** as an off-white solid (394 mg, 0.82 mmol, 89% yield).

**<sup>1</sup>H NMR** (400 MHz, DMSO-*d*<sub>6</sub>): δ 9.96 (s, 1H), 7.95 (br d, *J* = 7.8 Hz, 1H), 7.54 (d, *J* = 8.6 Hz, 2H), 7.24 (d, *J* = 8.6 Hz, 2H), 6.74 (br d, *J* = 8.8 Hz, 1H), 5.96 (t, *J* = 5.9 Hz, 1H), 5.39 (s, 2H), 5.07 (t, *J* = 5.6 Hz, 1H), 4.44 (d, *J* = 5.6 Hz, 3H), 3.84 (br t, *J* = 7.7 Hz, 1H), 3.10 - 2.99 (m, 1H), 2.99 - 2.90 (m, 1H), 2.03 - 1.92 (m, 1H), 1.77 - 1.66 (m, 1H), 1.65 - 1.53 (m, 1H), 1.51 - 1.31 (m, 11H), 0.87 (d, *J* = 6.8 Hz, 3H), 0.83 (d, *J* = 6.6 Hz, 3H).

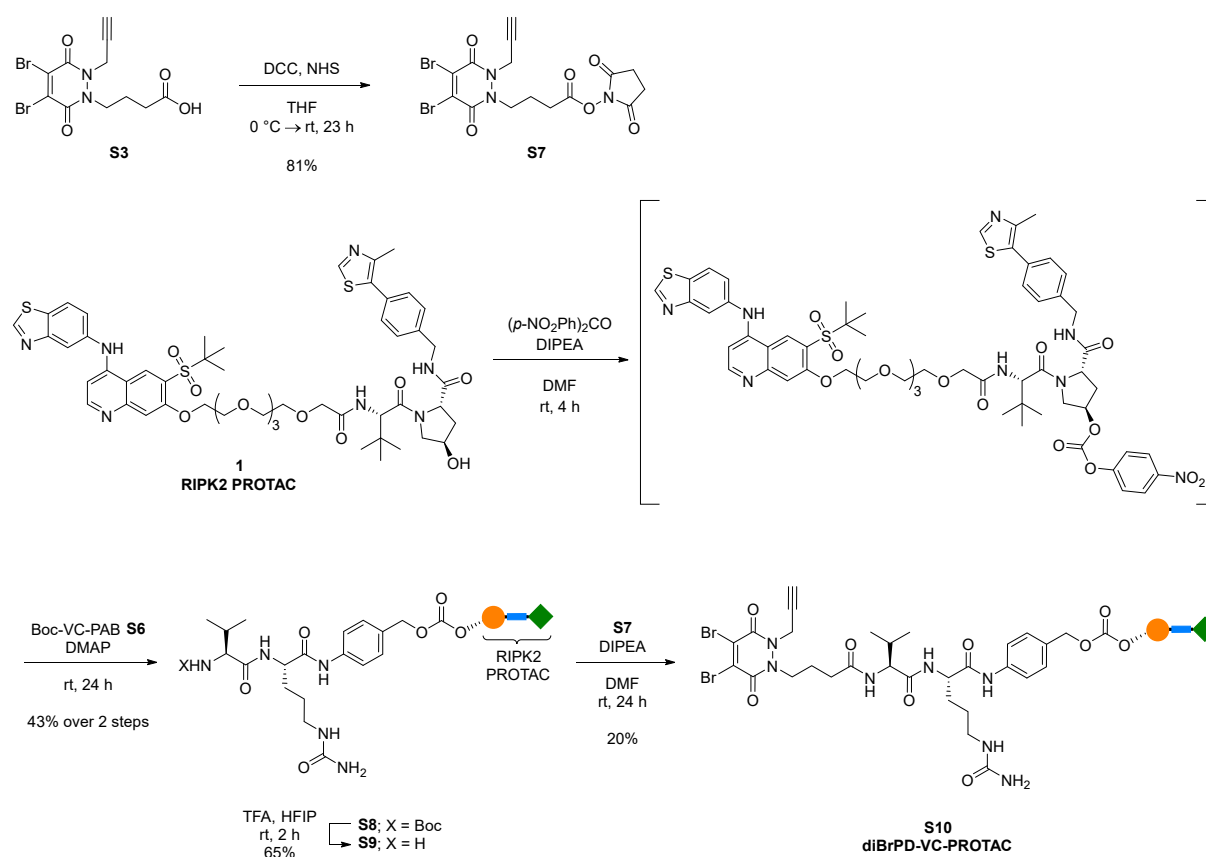
**<sup>13</sup>C NMR** (101 MHz, DMSO-*d*<sub>6</sub>): δ 171.8, 170.8, 159.3, 156.0, 137.95, 137.92, 127.4, 119.4, 78.6, 63.1, 60.2, 53.4, 39.1, 30.9, 30.2, 28.7, 27.2, 19.7, 18.6.

**LCMS** (High pH): *t*<sub>R</sub> = 0.75 min, [M+H]<sup>+</sup> 480.3, (100% purity).

**HRMS** (ESI): calculated for C<sub>23</sub>H<sub>38</sub>N<sub>5</sub>O<sub>6</sub> (*m/z*) [M+H]<sup>+</sup> requires 480.2822, found 480.2820 (error -0.4 ppm).

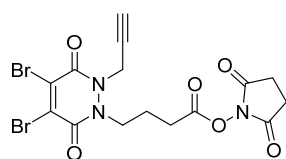
**IR** *v*<sub>max</sub> (neat): 3453, 3301 2965, 2915, 2871, 1692, 1634, 1600, 1527, 1449 cm<sup>-1</sup>.

## 1.5 Conjugation reagent: diBrPD-VC-PABC-PROTAC **S10**



**Scheme S3.** Synthesis of conjugation reagent diBrPD-VC-PABC-PROTAC **S10**.

### 2,5-Dioxopyrrolidin-1-yl 4-(4,5-dibromo-3,6-dioxo-2-(prop-2-yn-1-yl)-3,6-dihydropyridazin-1(2H)-yl)butanoate (**S7**)



A solution of **S3** (269 mg, 0.68 mmol) in THF (8.5 mL) was cooled to 0 °C and to this was added DCC (155 mg, 0.75 mmol). The mixture was stirred at 0 °C for 30 min, then *N*-hydroxysuccinimide (86 mg, 0.75 mmol) was added and the resulting mixture stirred at rt for 23 h. The suspension was filtered and the filtrate concentrated *in vacuo*. The residue was purified by column chromatography, eluting 20-80% EtOAc in cyclohexane on a 24 g silica column. Fractions containing product were combined and concentrated *in vacuo* to afford **S7** as a white solid (271 mg, 0.55 mmol, 81% yield).

$^1\text{H NMR}$  (400 MHz,  $\text{CDCl}_3$ ):  $\delta$  4.94 (d,  $J = 2.5$  Hz, 2H), 4.33 - 4.22 (m, 2H), 2.84 (s, 4H), 2.76 (t,  $J = 6.9$  Hz, 2H), 2.42 (t,  $J = 2.5$  Hz, 1H), 2.20 - 2.11 (m, 2H).

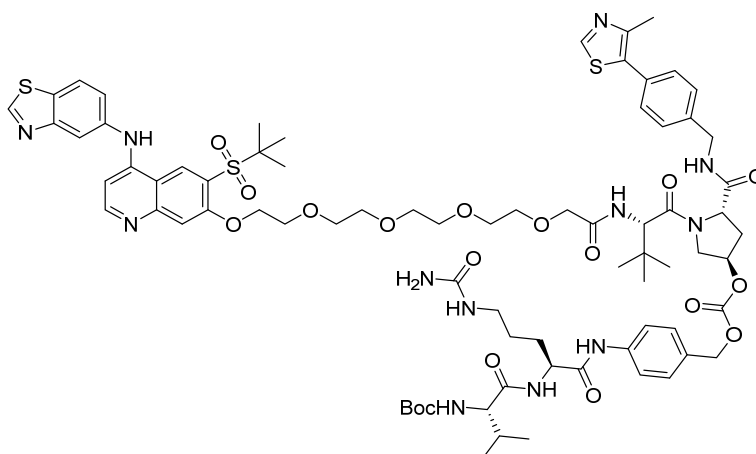
$^{13}\text{C}$  NMR (101 MHz,  $\text{CDCl}_3$ ):  $\delta$  168.8, 167.9, 153.5, 153.1, 136.8, 135.5, 75.6, 75.0, 46.5, 37.2, 28.0, 25.6, 22.7.

LCMS (Formic):  $t_R = 0.82$  min,  $[\text{M}(\text{Br}^{79}\text{Br}^{79})+\text{H}]^+$  489.8,  $[\text{M}(\text{Br}^{79}\text{Br}^{81})+\text{H}]^+$  491.8,  $[\text{M}(\text{Br}^{81}\text{Br}^{81})+\text{H}]^+$  493.8, (98% purity).

HRMS (ESI): calculated for  $\text{C}_{15}\text{H}_{14}\text{Br}_2\text{N}_3\text{O}_6$  ( $m/z$ )  $[\text{M}+\text{H}]^+$  requires 489.9249, found  $[\text{M}+\text{H}]^+$  489.9263 (error 2.4 ppm).

IR  $\nu_{\text{max}}$  (neat): 3261, 2946, 1812, 1780, 1731, 1634, 1575  $\text{cm}^{-1}$ .

***Tert*-butyl(((*S*)-1-(((*S*)-1-((4-((((3*R*,5*S*)-1-((*S*)-17-((4-(benzo[*d*]thiazol-5-ylamino)-6-(*tert*-butylsulfonyl)quinolin-7-yl)oxy)-2-(*tert*-butyl)-4-oxo-6,9,12,15-tetraoxa-3-azaheptadecanoyl)-5-((4-(4-methylthiazol-5-yl)benzyl)carbamoyl)pyrrolidin-3-yl)oxy)carbonyl)oxy)methyl)phenyl)amino)-1-oxo-5-ureidopentan-2-yl)amino)-3-methyl-1-oxobutan-2-yl)carbamate (**S8**)**



To a solution of **1** (100 mg, 0.094 mmol) in DMF (1 mL) was added bis(4-nitrophenyl)carbonate (72 mg, 0.24 mmol) and DIPEA (0.028 mL, 0.16 mmol) and the resulting mixture stirred at rt for 4 h. **S6** (68 mg, 0.14 mmol) and DMAP (12 mg, 0.094 mmol) was added and the resulting solution stirred at rt for 24 h. The solution was purified by reverse phase chromatography on an XSelect CSH Prep C18 5  $\mu\text{m}$  OBD column, eluting 30-85% acetonitrile in water with a 10 mM ammonium bicarbonate modifier adjusted to pH 10. Fractions containing product were combined and concentrated *in vacuo* to afford **S8** as a yellow amorphous solid (63 mg, 0.04 mmol, 43% yield).

$^1\text{H}$  NMR (400 MHz,  $\text{DMSO}-d_6$ ):  $\delta$  10.09 (s, 1H), 9.67 (s, 1H), 9.43 (s, 1H), 8.97 (s, 1H), 8.95 (s, 1H), 8.62 (br t,  $J = 5.9$  Hz, 1H), 8.5 (d,  $J = 5.4$  Hz, 1H), 8.2 (d,  $J = 8.6$  Hz, 1H), 8.04 (d,  $J = 2$  Hz, 1H), 7.99 (br d,  $J = 7.6$  Hz, 1H), 7.61 (d,  $J = 8.6$  Hz, 2H), 7.54 (dd,  $J = 8.6, 2$  Hz, 1H), 7.48 (s, 1H), 7.45 - 7.37 (m, 5H), 7.33 (d,  $J = 8.8$  Hz, 2H), 6.9 (d,  $J = 5.6$  Hz, 1H), 6.72 (br d,  $J = 8.8$  Hz, 1H), 5.96 (br t,  $J = 5.8$  Hz, 1H), 5.39 (s,

2H), 5.24 (br s, 1H), 5.1 (d, J = 12.5 Hz, 1H), 5.08 (d, J = 12 Hz, 1H), 4.51 - 4.22 (m, 8H), 4.04 (br d, J = 12.2 Hz, 1H), 3.95 (s, 2H), 3.90 - 3.78 (m, 3H), 3.63 - 3.50 (m, 12H), 3.09 - 2.99 (m, 1H), 2.99 - 2.90 (m, 1H), 2.44 (s, 3H), 2.37 - 2.29 (m, 1H), 2.20 - 2.10 (m, 1H), 2.01 - 1.91 (m, 1H), 1.75 - 1.65 (m, 1H), 1.65 - 1.54 (m, 1H), 1.47 - 1.35 (m, 11H), 1.33 (s, 9H), 0.96 (s, 9H), 0.86 (d, J = 6.9 Hz, 3H), 0.82 (d, J = 6.9 Hz, 3H).

<sup>13</sup>C NMR (151 MHz, DMSO-*d*<sub>6</sub>): δ 171.8, 171.4, 171.1, 169.7, 169.4, 159.3, 157.8, 156.8, 155.9, 154.6, 154.5, 154.2, 153.5, 151.9, 149.9, 148.2, 139.7, 139.5, 139.2, 131.6, 131.2, 130.4, 130.2, 129.7, 129.6, 129.2, 127.9, 123.6, 123.5, 122.2, 119.5, 117.2, 113.8, 110.8, 101.8, 78.6, 77.4, 70.9, 70.4, 70.31, 70.27, 70.1, 70.0, 69.5, 69.0, 68.8, 61.2, 60.2, 58.7, 56.5, 54.0, 53.4, 42.2, 39.1, 35.6, 35.2, 30.9, 30.0, 28.6, 27.2, 26.6, 24.2, 19.7, 18.6, 16.4.

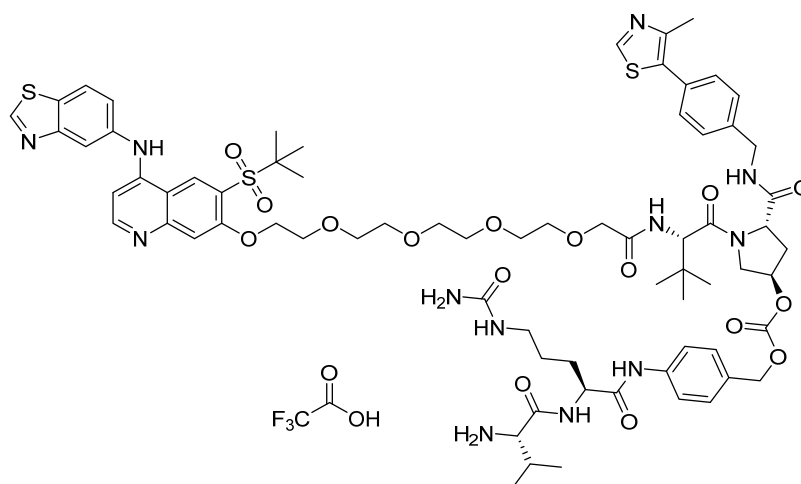
LCMS (High pH): *t*<sub>R</sub> = 1.21 min, ([M+2H]/2)<sup>+</sup> 783.6, (100% purity).

HRMS (ESI): calculated for C<sub>76</sub>H<sub>102</sub>N<sub>12</sub>O<sub>18</sub>S<sub>3</sub> (*m/z*) ([M+2H]/2)<sup>+</sup> requires 783.3299, found ([M+2H]/2)<sup>+</sup> 783.3311 (error 1.5 ppm).

IR *v*<sub>max</sub> (neat): 3278, 2932, 1728, 1635, 1572, 1522 cm<sup>-1</sup>.

[α<sub>D</sub>]<sup>20.0 °C</sup><sub>589 nm</sub> (*c* 1.00, MeOH): -16°

**4-((S)-2-((S)-2-Amino-3-methylbutanamido)-5-ureidopentanamido)benzyl ((3R,5S)-1-((S)-17-((4-(benzo[*d*]thiazol-5-ylamino)-6-(*tert*-butylsulfonyl)quinolin-7-yl)oxy)-2-(*tert*-butyl)-4-oxo-6,9,12,15-tetraoxa-3-azaheptadecanoyl)-5-((4-(4-methylthiazol-5-yl)benzyl)carbamoyl)pyrrolidin-3-yl) carbonate, trifluoroacetic acid salt (S9)**

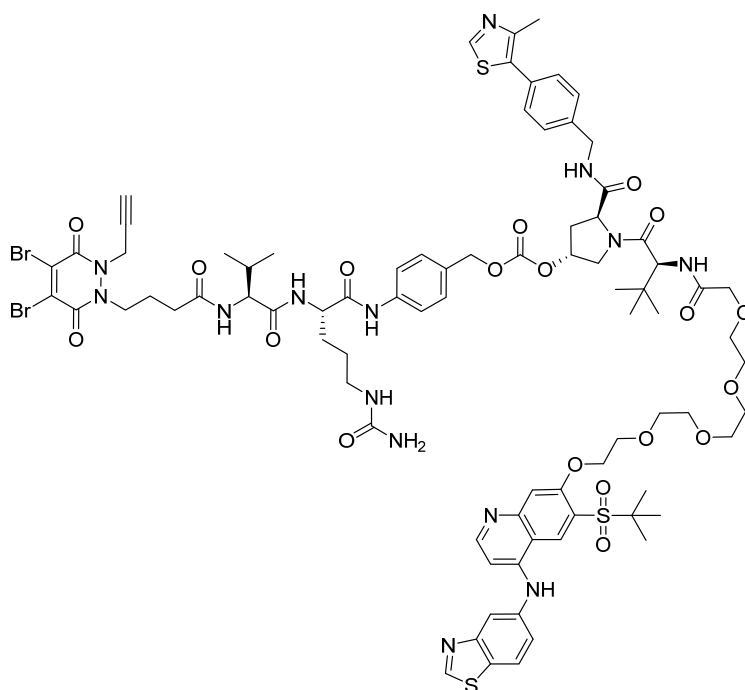


To a solution of **S8** (97 mg, 0.062 mmol) in HFIP (1 mL) was added TFA (48 μL, 0.62 mmol) and the resulting solution stirred at rt for 2 h. The reaction mixture was concentrated under a stream of N<sub>2</sub> to

afford **S9** as a yellow gum (98 mg, 0.04 mmol, 65% yield). The crude product was carried forward with no additional purification.

LCMS (Formic)  $t_R = 0.72$  min,  $([M+2H]/2)^+ 733.6$ , (67% purity).

**(3R,5S)-1-((S)-17-(((4-(Benzo[d]thiazol-5-ylamino)-6-(tert-butylsulfonyl)quinolin-7-yl)oxy)-2-(tert-butyl)-4-oxo-6,9,12,15-tetraoxa-3-azaheptadecanoyl)-5-(((4-(4-methylthiazol-5-yl)benzyl)carbamoyl)pyrrolidin-3-yl(4-((S)-2-((S)-2-(4-(4,5-dibromo-3,6-dioxo-2-(prop-2-yn-1-yl)-3,6-dihydropyridazin-1(2H)-yl)butanamido)-3-methylbutanamido)-5-ureidopentanamido)benzyl) carbonate (S10)**



**S7** (23 mg, 0.046 mmol) was added to a solution of **S9** (98 mg, 0.042 mmol) and DIPEA (11  $\mu$ l, 0.062 mmol) in DMF (500  $\mu$ l), and the resulting solution stirred at rt for 15 h. Additional DIPEA (11  $\mu$ l, 0.062 mmol) was added and the resulting solution stirred for another 9 h. The solution was purified directly by reverse phase chromatography on an XSelect CSH Prep C18 5  $\mu$ m OBD column, eluting 30-50% acetonitrile in water with a 10 mM ammonium bicarbonate modifier adjusted to pH 10. Fractions containing product were combined and concentrated under a stream of  $N_2$  to afford **S10** as a yellow solid (15 mg, 8.14  $\mu$ mol, 20% yield).

$^1H$  NMR (600 MHz,  $DMSO-d_6$ ):  $\delta$  9.98 (s, 1 H), 9.69 (br s, 1 H), 9.43 (s, 1 H), 8.97 (s, 1 H), 8.95 (s, 1 H), 8.62 (t,  $J = 6.1$  Hz, 1 H), 8.5 (d,  $J = 5.5$  Hz, 1 H), 8.2 (d,  $J = 8.4$  Hz, 1 H), 8.13 (d,  $J = 7.3$  Hz, 1 H), 8.04 (d,  $J = 1.1$  Hz, 1 H), 7.91 (d,  $J = 8.4$  Hz, 1 H), 7.62 (d,  $J = 8.8$  Hz, 2 H), 7.54 (dd,  $J = 8.6, 1.3$  Hz, 1 H), 7.48 (s, 1

H), 7.44 - 7.38 (m, 5 H), 7.33 (d,  $J = 8.8$  Hz, 2 H), 6.9 (d,  $J = 5.4$  Hz, 1 H), 5.96 (br t,  $J = 5.9$  Hz, 1 H), 5.39 (s, 2 H), 5.24 (br s, 1 H), 5.1 (d,  $J = 12.2$  Hz, 1 H), 5.07 (d,  $J = 12.1$  Hz, 1 H), 4.96 (dd,  $J = 18.3, 2.6$  Hz, 1 H), 4.92 (dd,  $J = 18.3, 2.6$  Hz, 1 H), 4.49 - 4.40 (m, 3 H), 4.40 - 4.36 (m, 1 H), 4.32 (br t,  $J = 4$  Hz, 2 H), 4.27 (dd,  $J = 15.8, 5.5$  Hz, 1 H), 4.22 (dd,  $J = 8.3, 6.8$  Hz, 1 H), 4.13 - 4.06 (m, 2 H), 4.04 (br d,  $J = 12.1$  Hz, 1 H), 3.95 (s, 2 H), 3.86 (br dd,  $J = 11.9, 3.9$  Hz, 1 H), 3.84 - 3.81 (m, 2 H), 3.63 - 3.51 (m, 12 H), 3.46 (t,  $J = 2.4$  Hz, 1 H), 3.06 - 2.99 (m, 1 H), 2.99 - 2.92 (m, 1 H), 2.44 (s, 3 H), 2.33 (m, 1 H), 2.31 - 2.21 (m, 2 H), 2.15 (ddd,  $J = 13.9, 9.2, 4.8$  Hz, 1 H), 1.98 (dspt,  $J = 6.9, 6.7$  Hz, 1 H), 1.85 (quin,  $J = 7.3$  Hz, 2 H), 1.75 - 1.68 (m, 1 H), 1.65 - 1.57 (m, 1 H), 1.50 - 1.42 (m, 1 H), 1.41 - 1.35 (m, 1 H), 1.33 (s, 9 H), 0.96 (s, 9 H), 0.88 (d,  $J = 6.6$  Hz, 3 H), 0.85 (d,  $J = 6.6$  Hz, 3 H).

**$^{13}\text{C}$  NMR** (150 MHz, DMSO- $d_6$ ):  $\delta$  171.5, 171.1, 170.9, 170.6, 169.2, 168.9, 158.8, 157.3, 154.1, 153.9, 153.7, 153.1, 153.0, 152.9, 152.4, 151.3, 149.4, 147.7, 139.2, 139.1, 138.7, 136.2, 136.1, 134.8, 131.0, 130.7, 129.8, 129.7, 129.2, 129.1, 128.6, 127.4, 123.0, 121.6, 118.9, 116.7, 113.2, 110.2, 101.2, 77.0, 76.8, 76.4, 70.4, 69.82, 69.79, 69.7, 69.5, 69.4, 68.9, 68.5, 68.3, 60.7, 58.2, 57.7, 56.0, 53.5, 53.1, 46.7, 41.7, 38.6, 37.0, 35.1, 34.7, 31.4, 30.4, 29.1, 26.8, 26.0, 23.6, 23.2, 19.1, 18.1, 15.9.

**$^{15}\text{N}$  NMR**:  $\delta$  333, 314, 160, 155, 129, 117, 119, 113, 112, 94, 82, 73. Pyrrolidine and quinoline N's not observed.

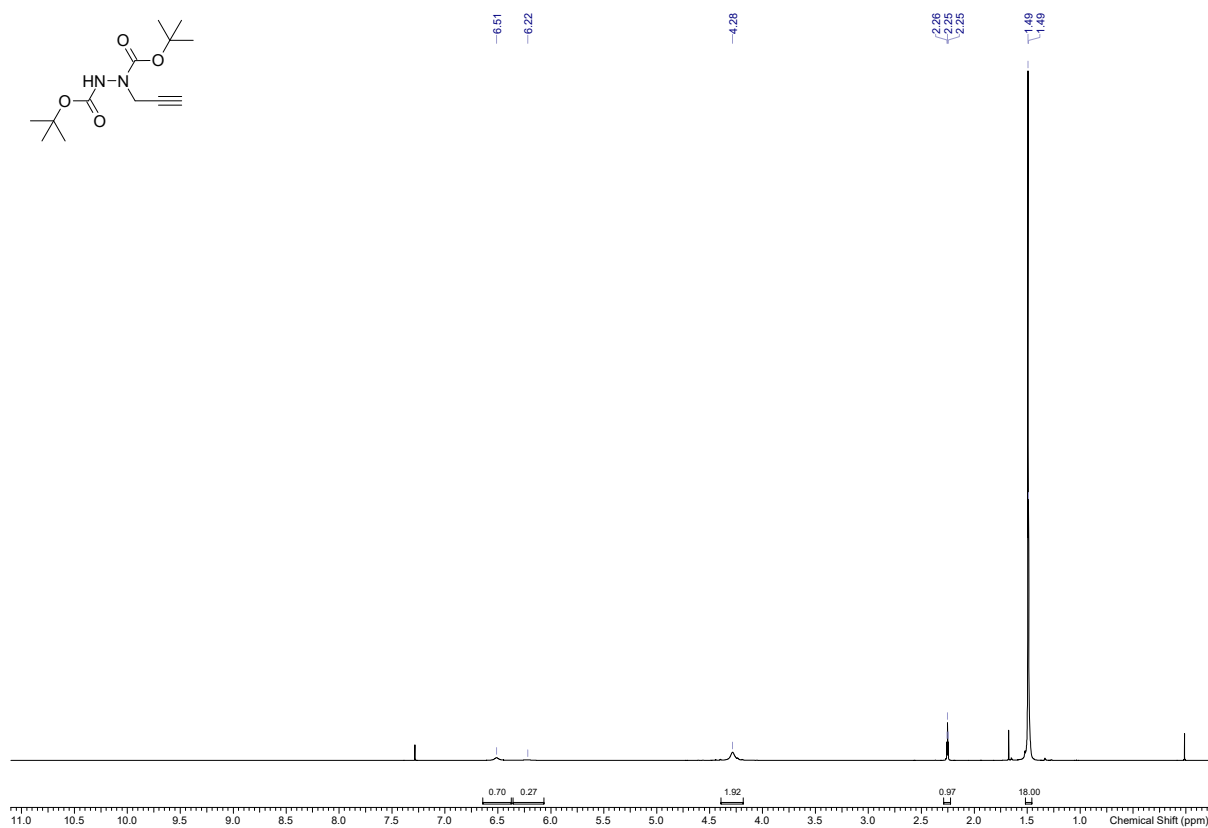
**LCMS** (High pH):  $t_R = 1.17$  min, ( $[\text{M}(^{79}\text{Br}^{79}\text{Br})+2\text{H}]/2$ )<sup>+</sup> 920.8, ( $[\text{M}(^{79}\text{Br}^{81}\text{Br})+2\text{H}]/2$ )<sup>+</sup> 921.4, ( $[\text{M}(^{81}\text{Br}^{81}\text{Br})+2\text{H}]/2$ )<sup>+</sup> 922.0, (93% purity).

**HRMS** (ESI): calculated for  $\text{C}_{82}\text{H}_{101}\text{Br}_2\text{N}_{14}\text{O}_{19}\text{S}_3$  ( $m/z$ )  $[\text{M}+\text{H}]^+$  requires 1839.4898, found 1839.4243 (error 0.5 ppm).

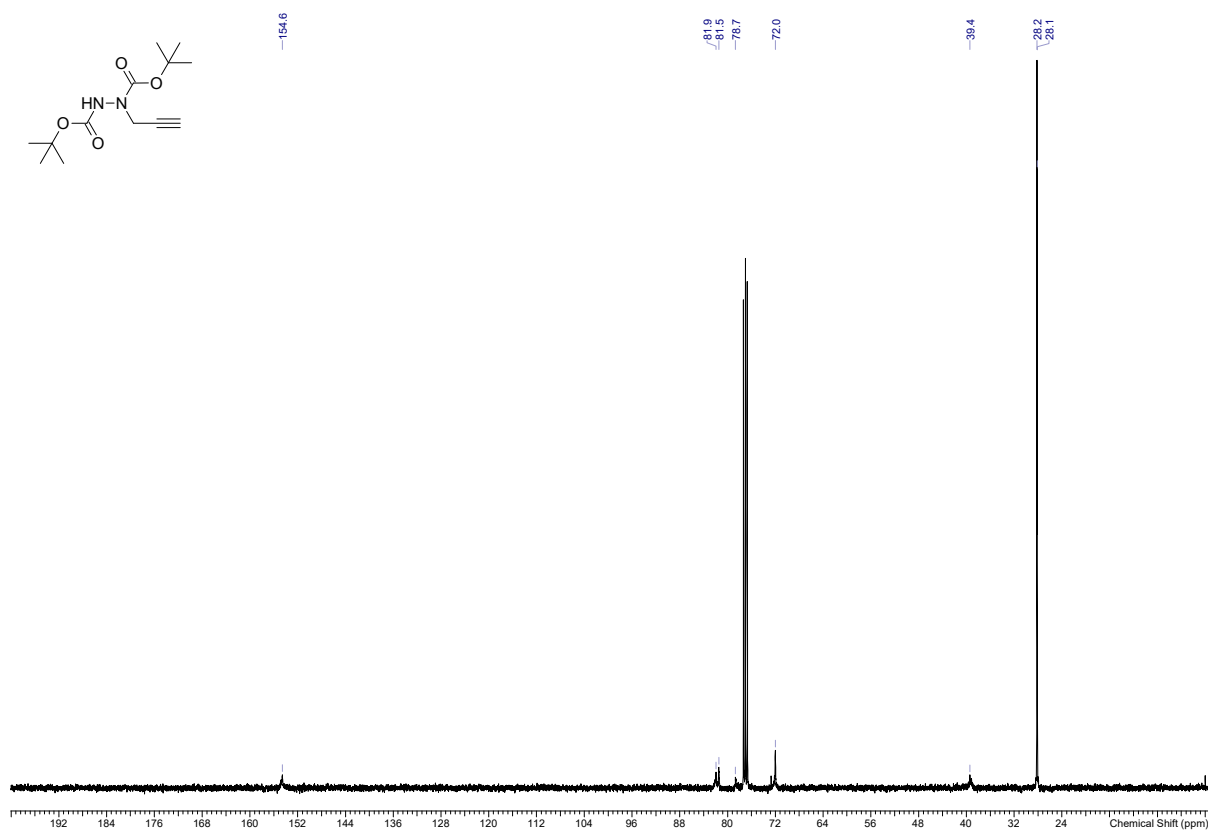
**IR  $\nu_{\text{max}}$  (neat)**: 3263, 2947, 1780, 1728, 1632, 1574, 1404  $\text{cm}^{-1}$ .

**$[\alpha_D]^{20.0}$**   $_{589\text{ nm}}$  ( $c$  0.5, DMSO):  $-16^\circ$

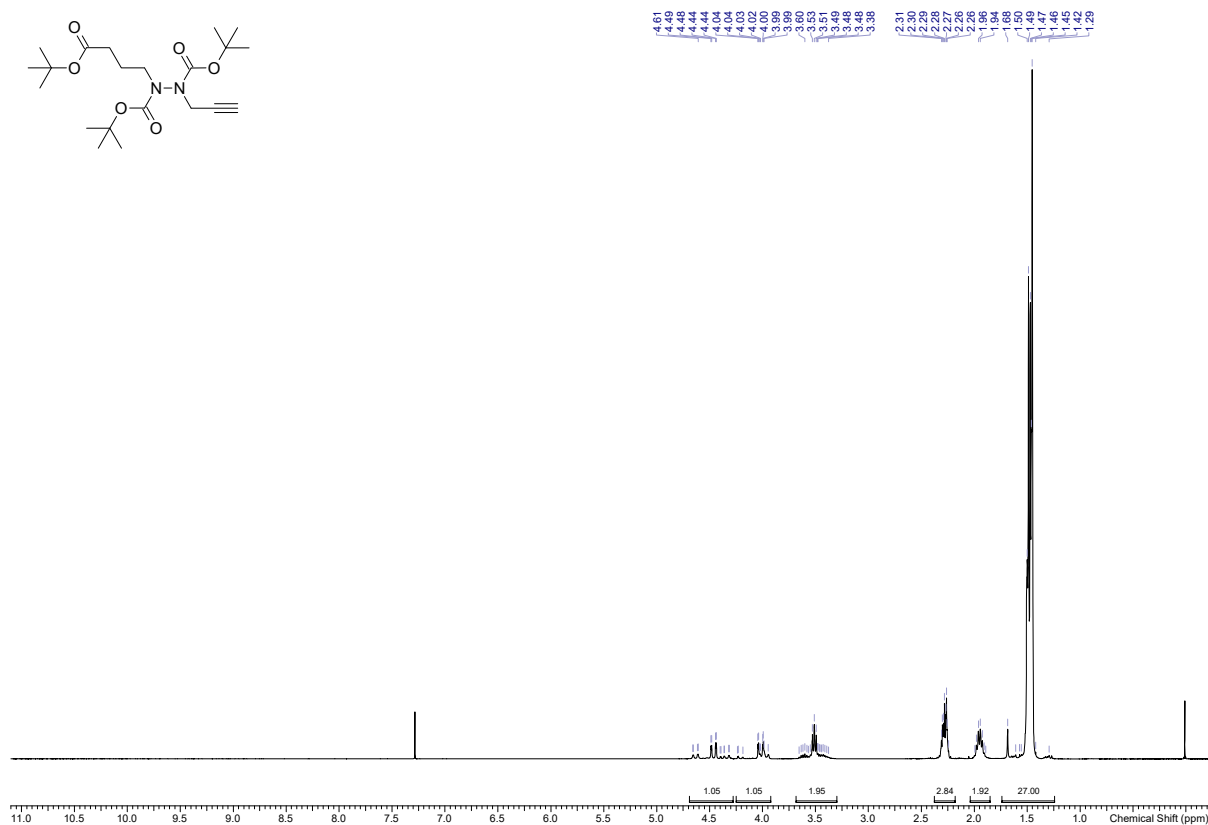
## 1.6 NMR Spectra



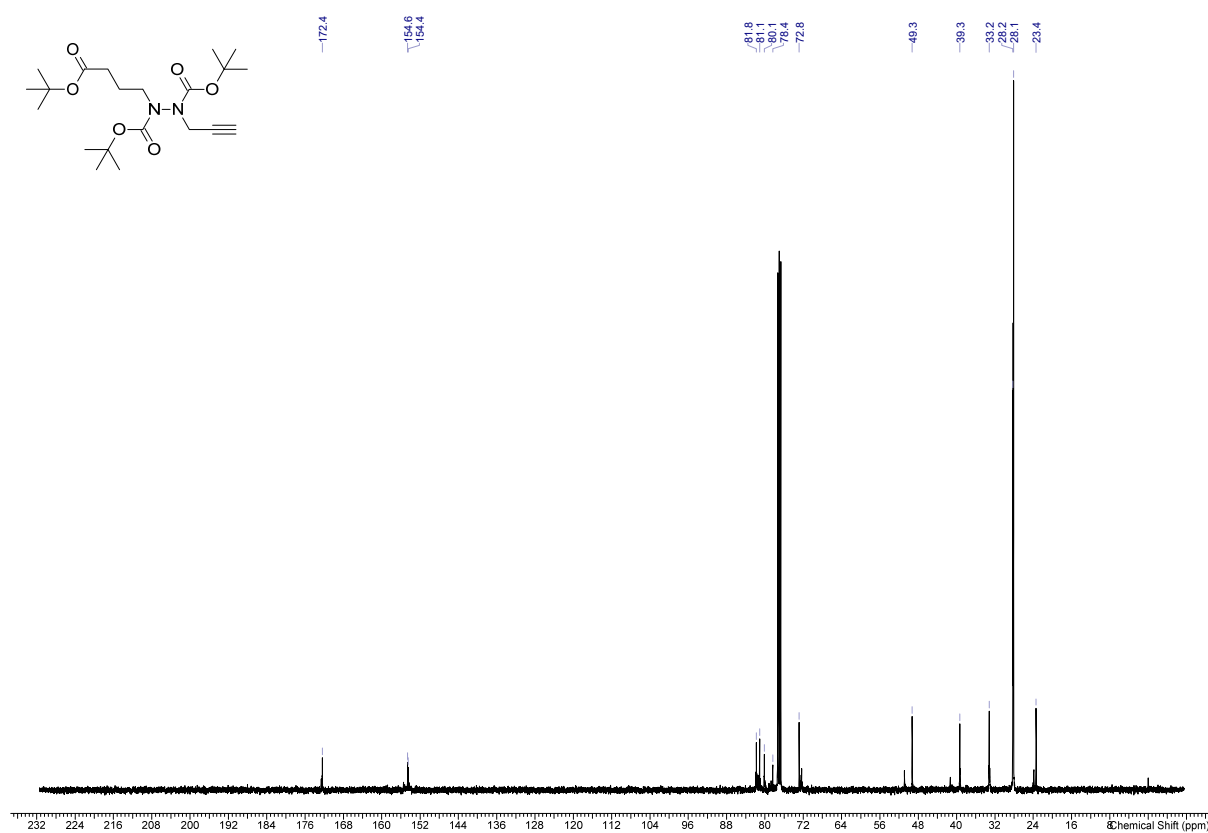
H NMR of S1.



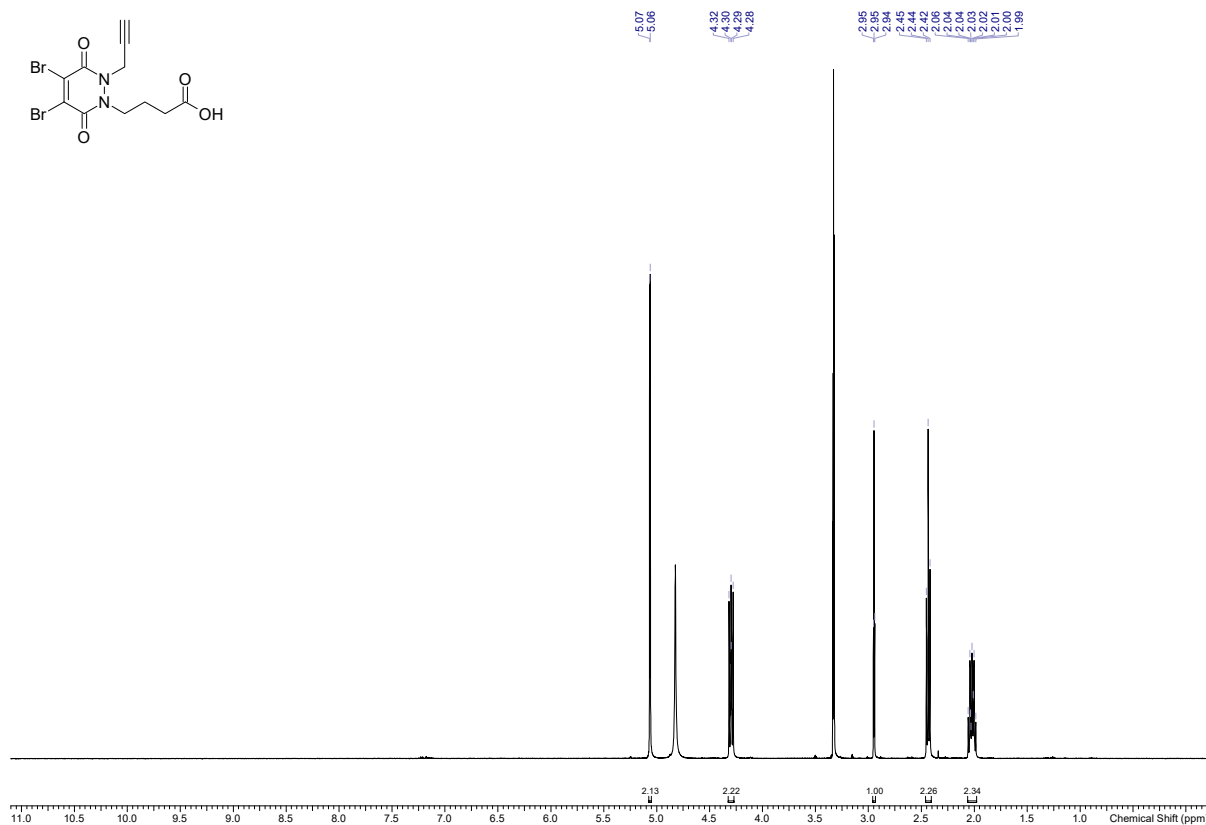
C NMR of S1.



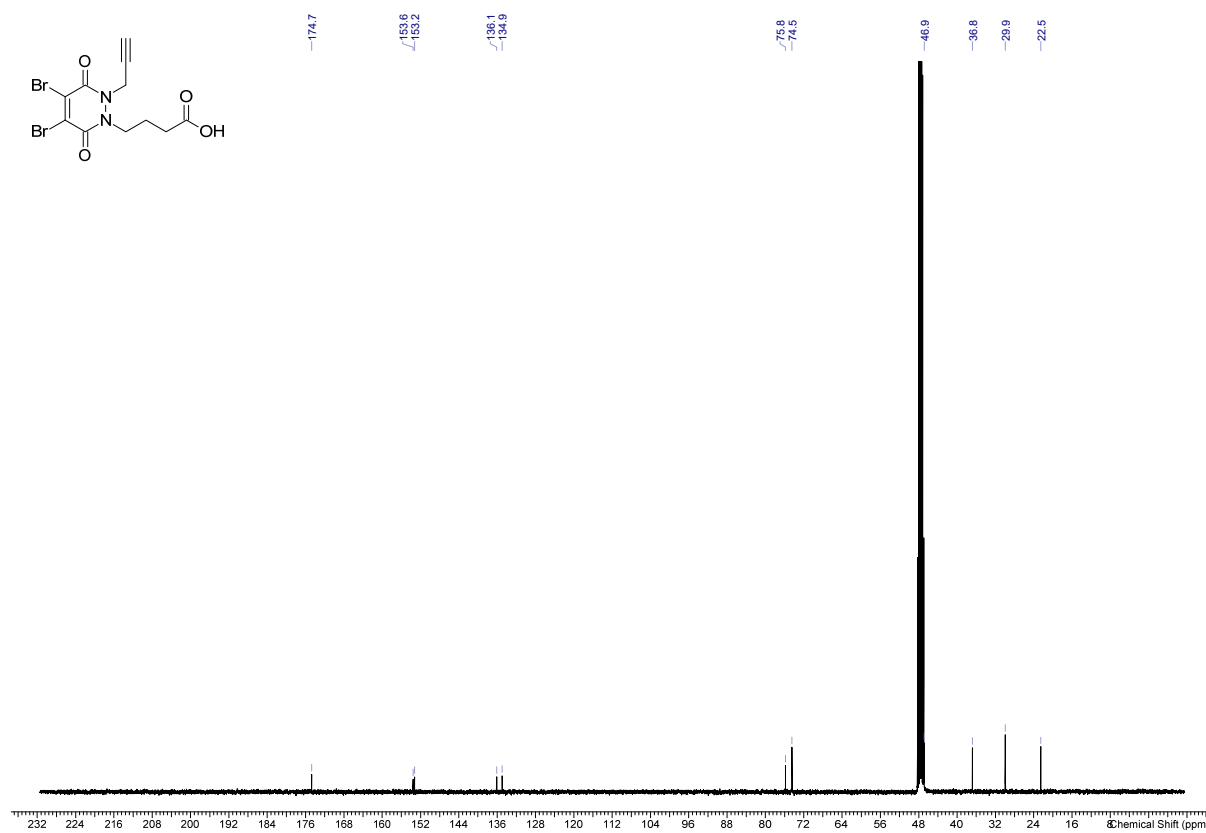
**H NMR of S2.**



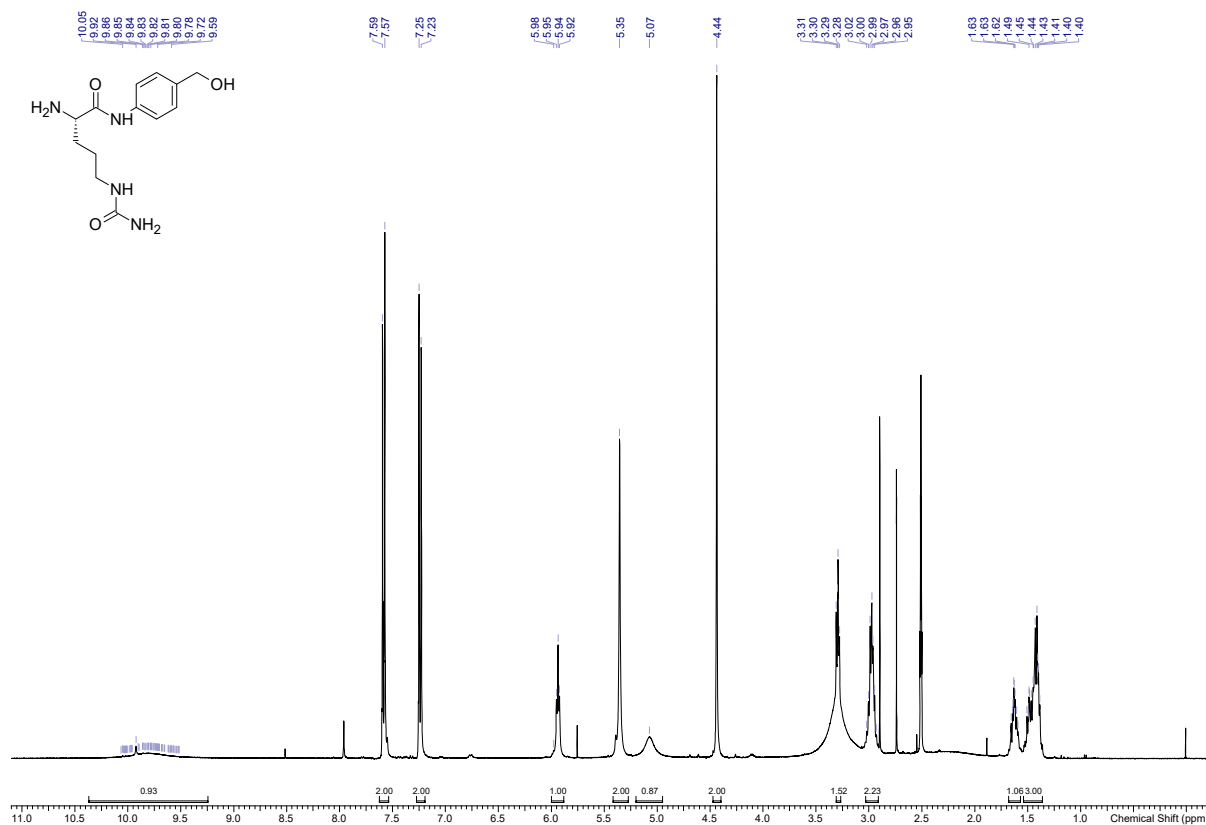
**C NMR of S2.**



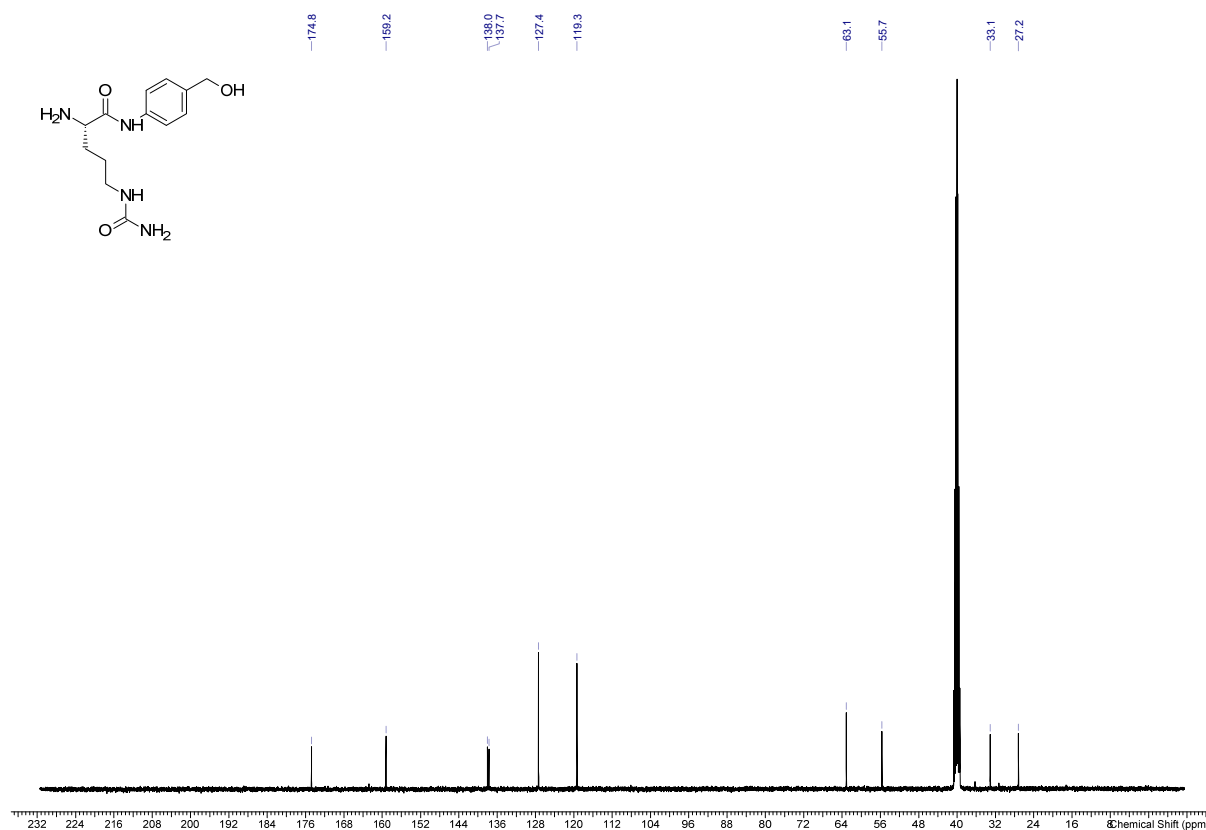
H NMR of S3.



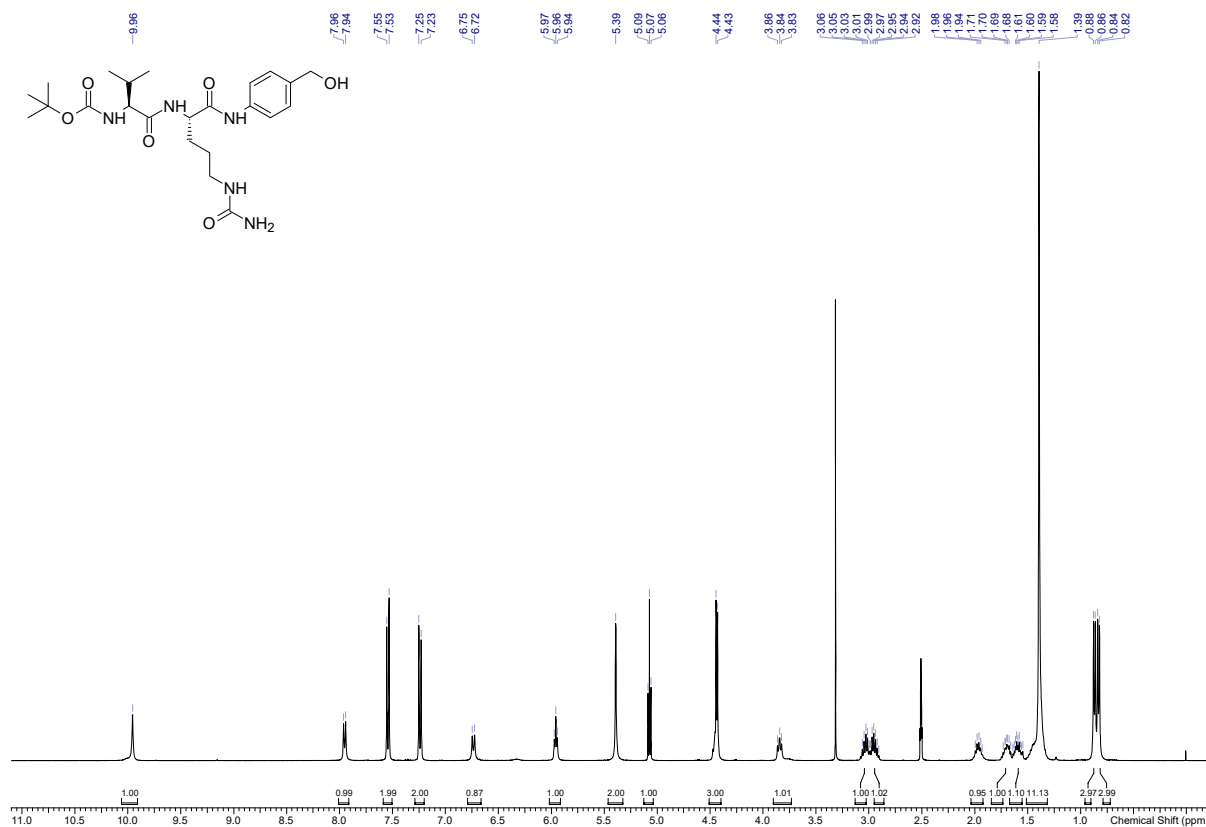
C NMR of S3.



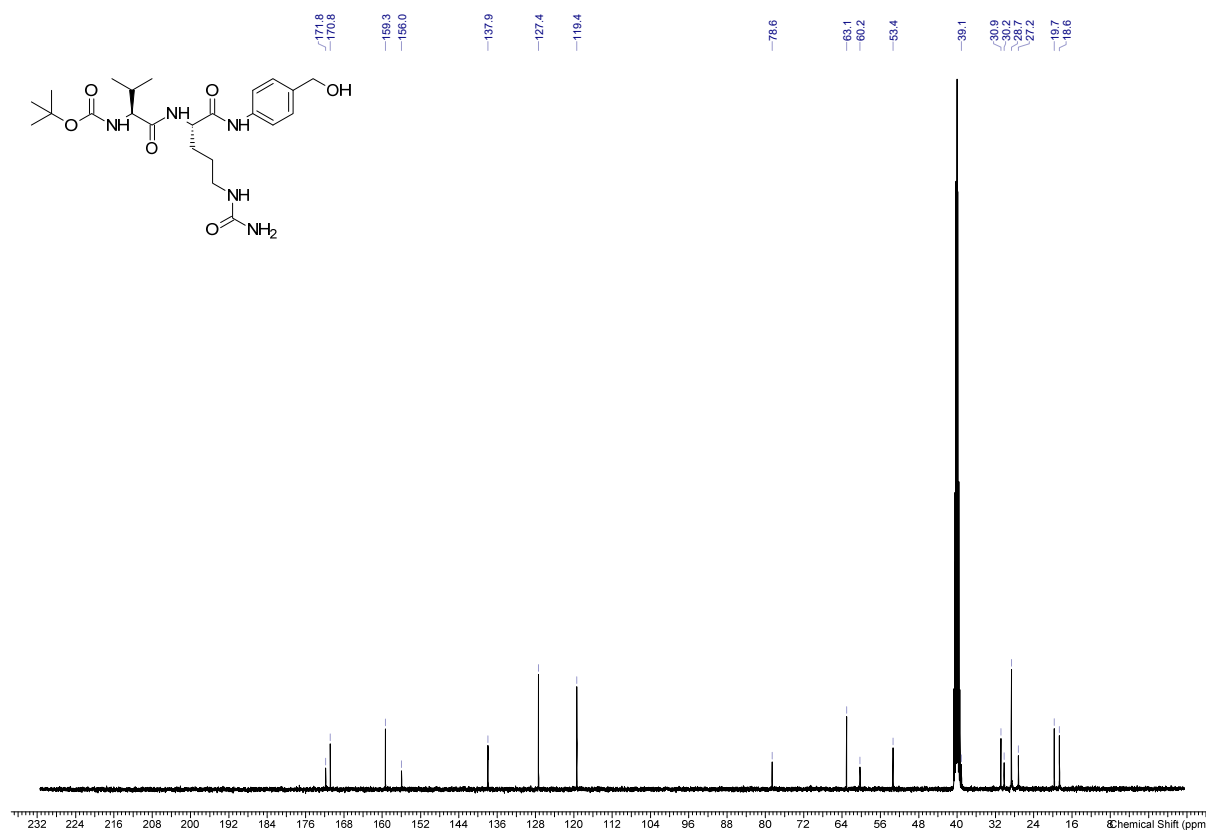
**H NMR of S5.**



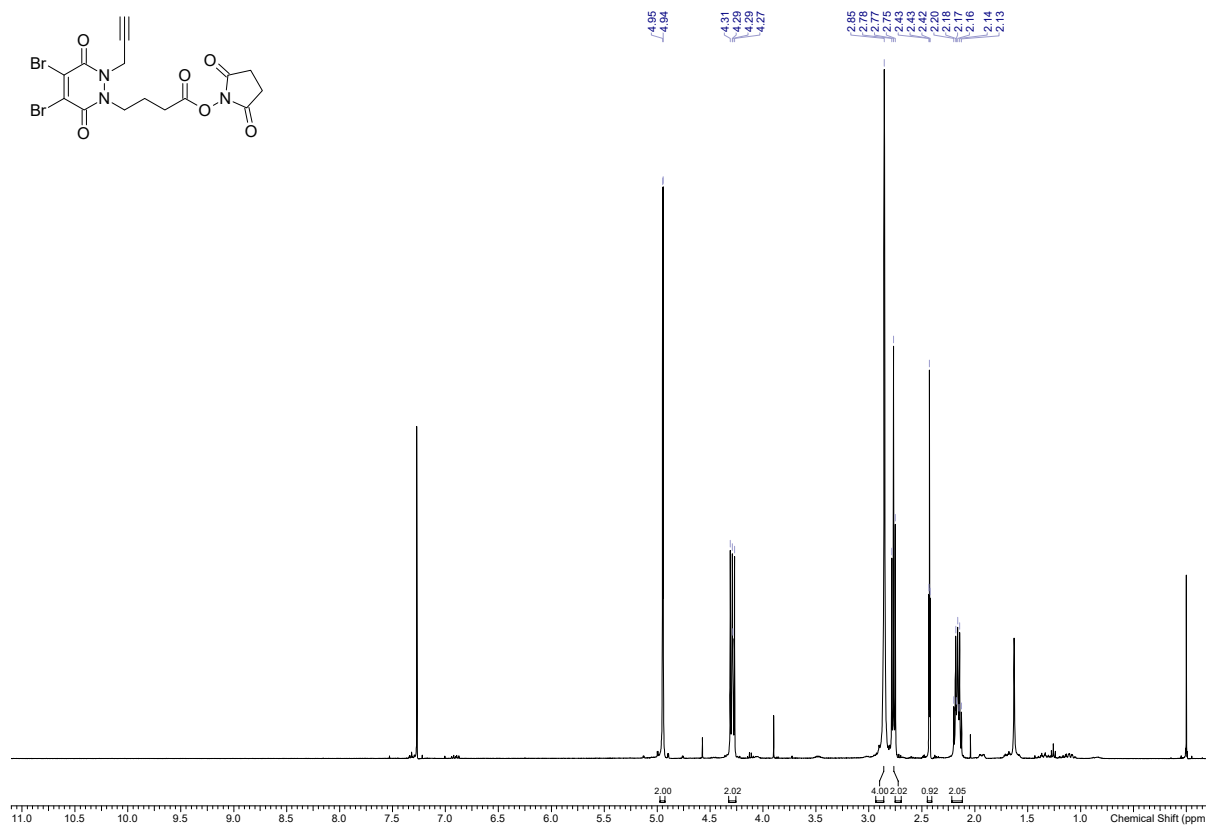
**C NMR of S5.**



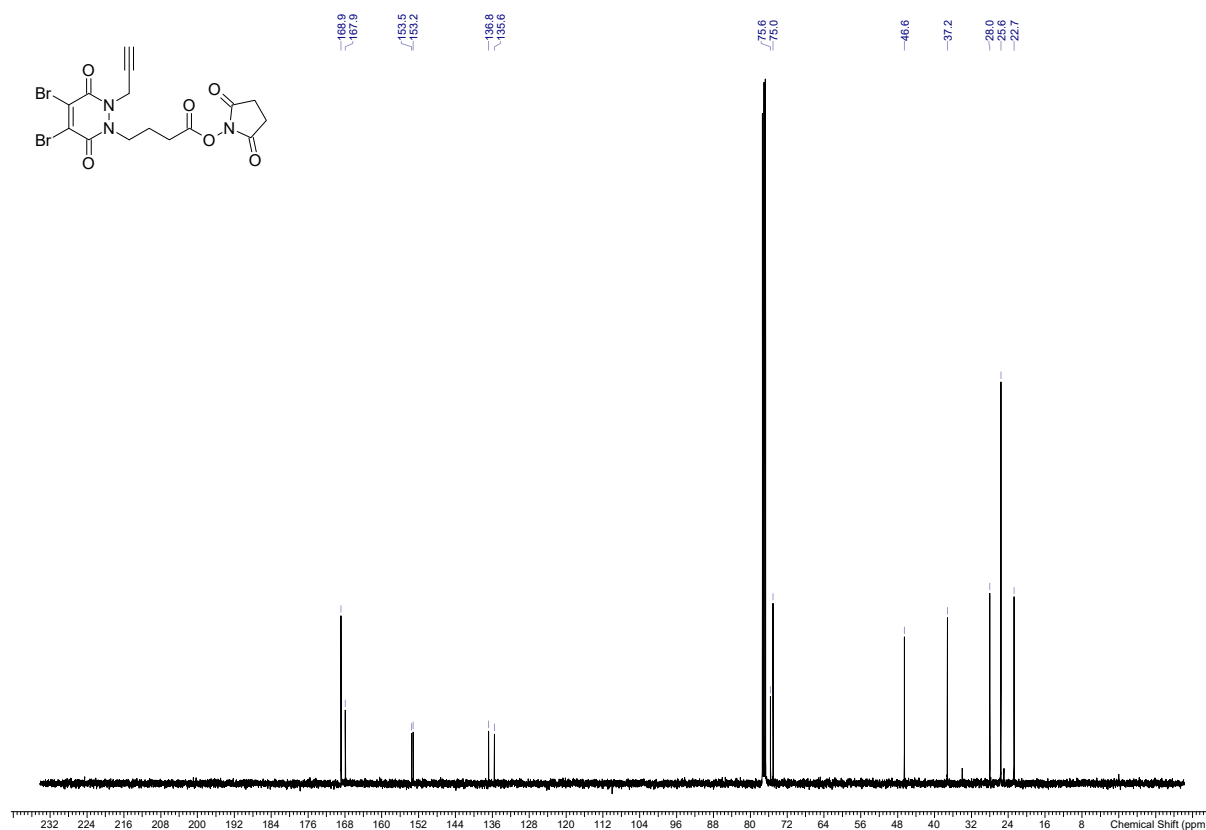
**H NMR of S6.**



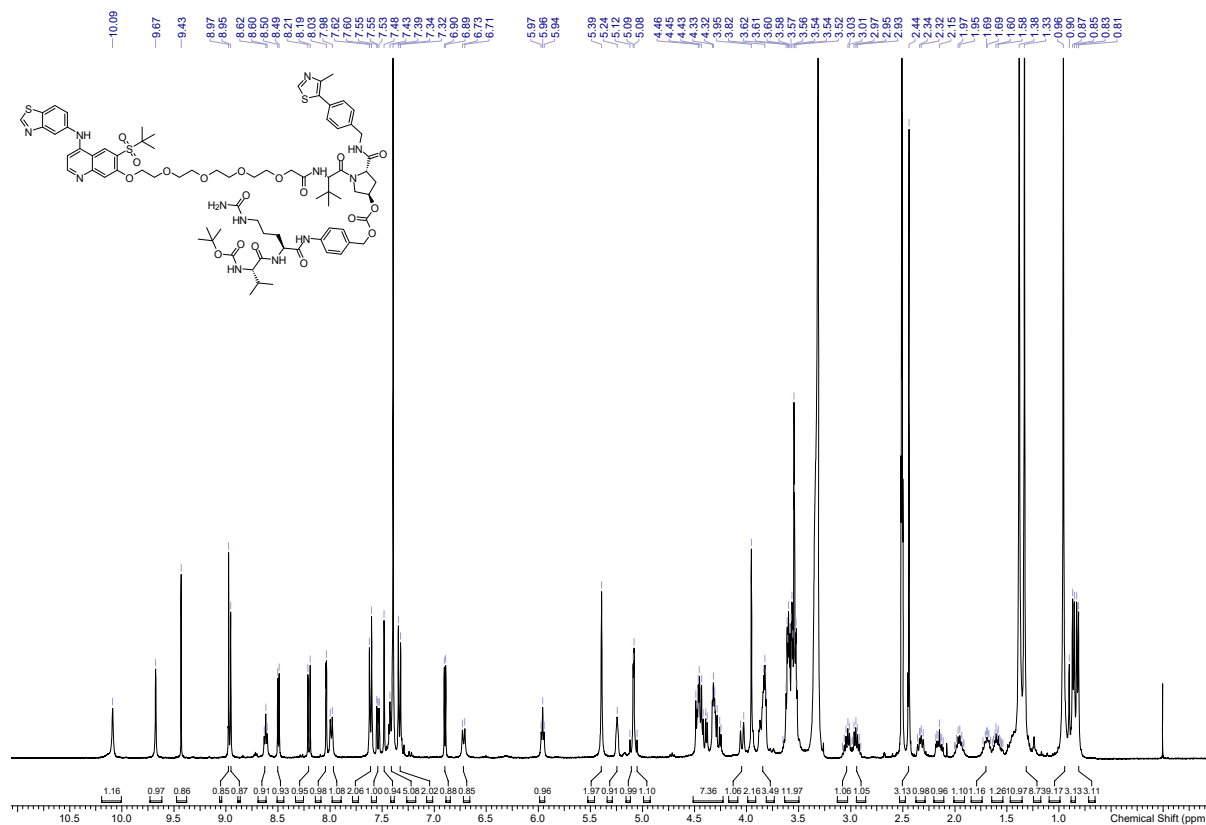
**C NMR of S6.**



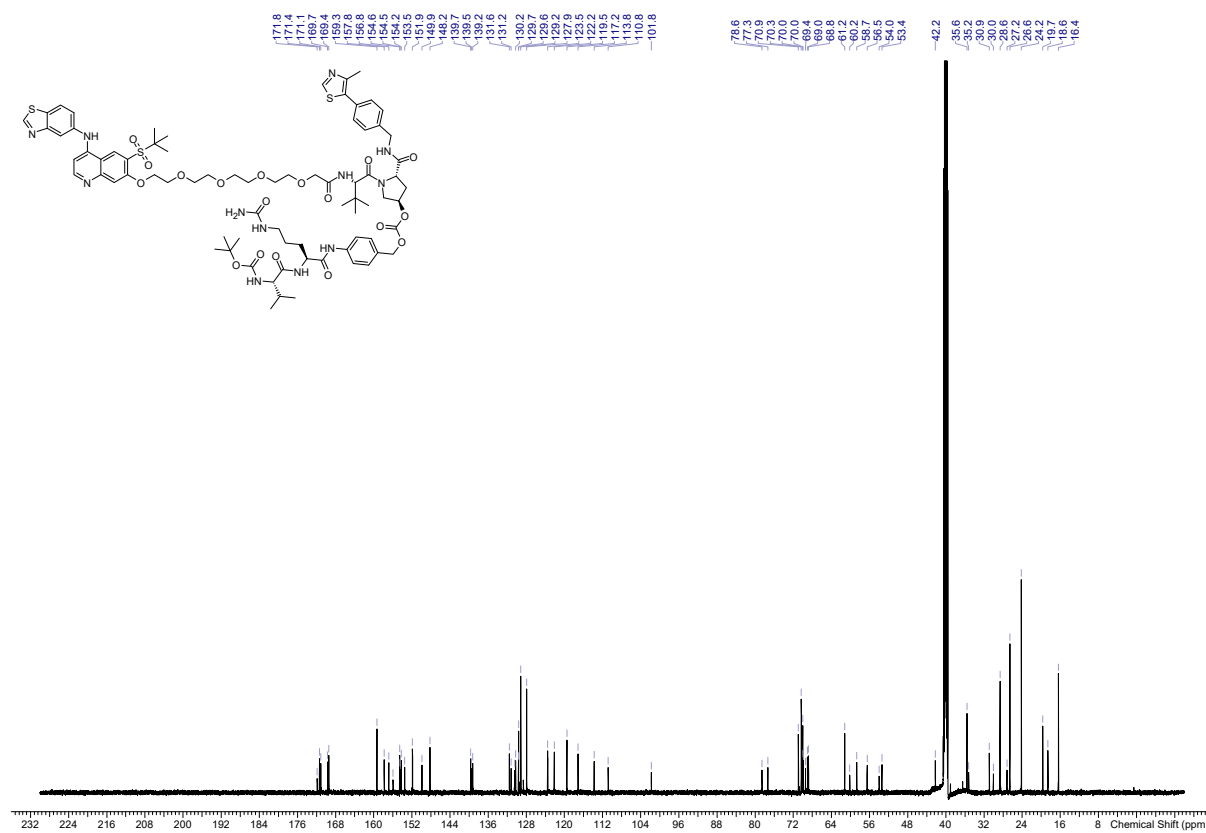
**H NMR of S7.**



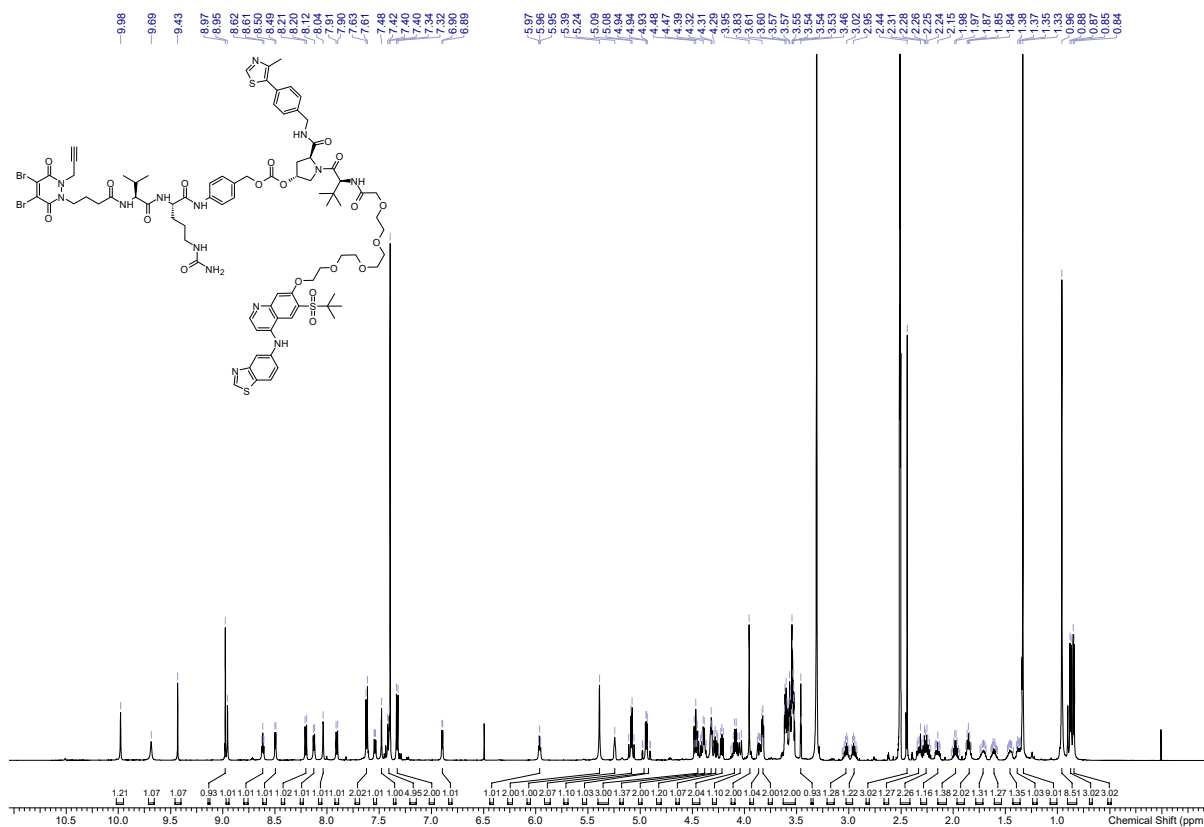
**C NMR of S7.**



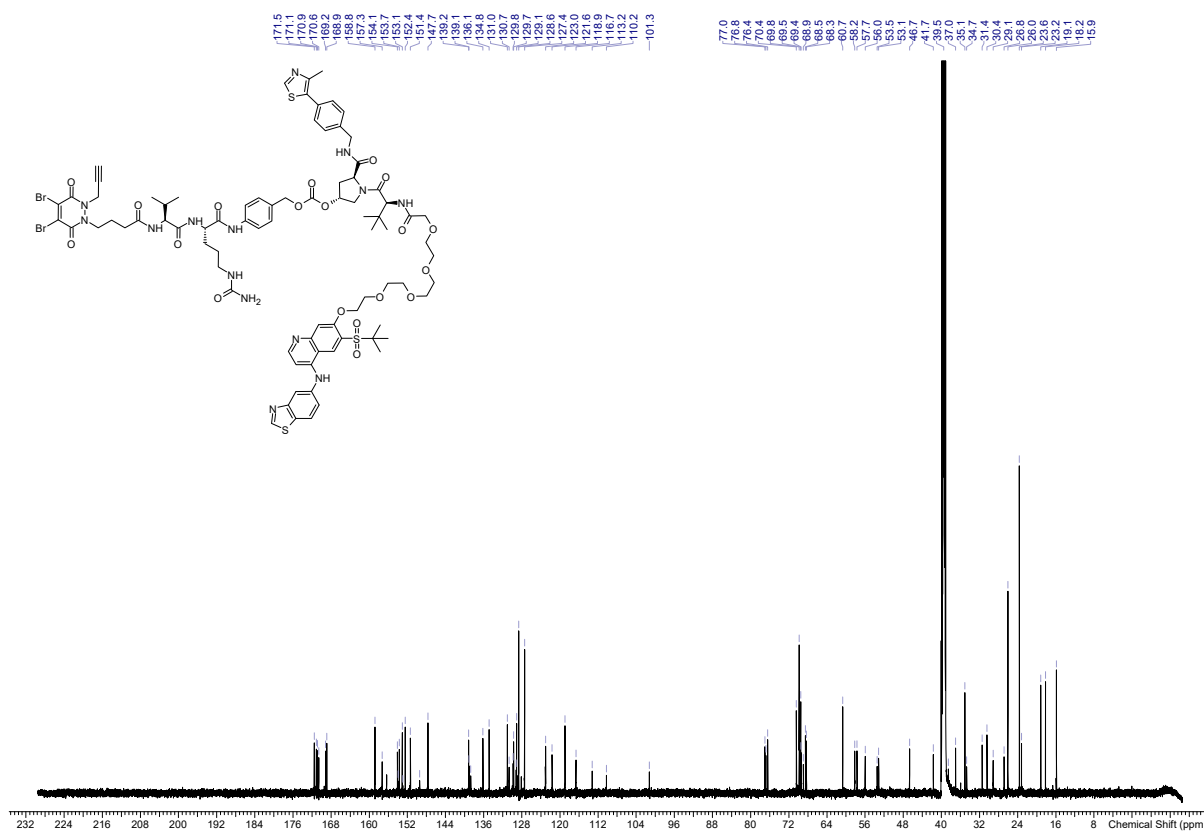
**H NMR of S8.**



**C NMR of S8.**



H NMR of S10.



C NMR of S10.

## 2. Biology and Bioconjugation

### 2.1 Materials and methods

Solvents and reagents were purchased from commercial suppliers and used as received. Phosphate-buffered saline (PBS): 2.67 mM KCl, 1.5 mM KH<sub>2</sub>PO<sub>4</sub>, 138 mM NaCl, Na<sub>2</sub>HPO<sub>4</sub>·7H<sub>2</sub>O. Borate-buffered saline (BBS): 50 mM Boric acid, 50 mM NaOH, 50 mM NaCl, 5 mM EDTA, adjusted to pH 8.5 with HCl. Conjugation experiments were carried out in standard polypropylene Eppendorf safe-lock tubes (1.5 mL) at atmospheric pressure and the temperature stated.

#### Centrifugation

Centrifugation was carried out in either an Eppendorf 5417R centrifuge or a Sorvall Legend XTR centrifuge. Ultrafiltration was carried out using either Merck Millipore Amicon (30,000 Da membrane) or VivaSpin 5000 concentrators (10,000 or 30,000 Da MwCO).

#### Protein concentration

Protein concentration was determined by measuring the absorbance at  $\lambda = 280$  nm using a NanoDrop 1000 spectrophotometer.

#### Intact Mass Spectrometry (Intact MS)

Intact MS was performed using a Waters Acquity UPLC pump system connected with a TUV detector with Acquity RDa Waters Mass Spectrometer and using column: Waters BioResolve 2.1x50mm column. Mobile phase A was Water + 0.1% Formic acid, mobile phase B was MeCN + 0.1% Formic acid. The sample was run at a flow rate of 0.5 ml/min. The obtained m/z spectra was deconvoluted and analysed using the Unifi Version 1.9.4.053.

#### Gel Electrophoresis

SDS-PAGE was carried out using Invitrogen NuPage 4-12% Bis-Tris gels. Samples were mixed with SDS non-reducing loading buffer (NuPAGE LDS sample buffer 4x) or reducing loading buffer (NuPAGE LDS sample buffer + 0.5 M DTT in a 9:1 ratio). Reduced samples were heated at 90 °C for 5 min before being loaded onto the gel. Samples were run at a constant current (120 mA) and voltage (200 V) for 40 min in Novex NuPage MES SDS running buffer (20x). Gels were stained with InstantBlue® Coomassie protein stain and de-stained with H<sub>2</sub>O. The molecular ladder used was either the SeeBlue Plus 2 pre-stained protein standard or Novex Sharp pre-stained protein standard.

#### Gel imaging

Gel imagery was obtained using a BioRad Geldoc™ EZ Imager (White Light Sample Tray) and processed using Image Lab: Exposure Time (sec) 0.273 (Auto - Intense Bands), Application Instant Blue,

Dark Type Referenced, Ref. Bkgd. Time (sec) 10, Flat Field Applied, Serial Number 735BR07211, Software Version 6.1.0.07, Illumination Mode White Transillumination.

## 2.2 Expression of mAbs

mAbs were generated from HEK293 cells transfected with 1 mg of mAb DNA (0.5 mg HC + 0.5 mg LC). The media consisted of BalanCD, GlutaMAX, geneticin and 1 mg of mAb in 100 mL of OptiMEM (HEPES, 2.4 g/L sodium bicarbonate, L-Gln). The total volume was 1 L with a cell concentration was  $1.58 \times 10^6$  cells/mL. The mixture was incubated at 37 °C for 6 days on a shaking platform at 125 rpm and 5% CO<sub>2</sub>. After 48 h, cells were treated with tryptone (25 mL). After 72 h, cells were treated with 3 M fructose (33 mL). After 6 days, the mixture was spun at 4000 rpm for 15 min and the supernatant filtered through a Nalgene Rapid-Flow 90 mm Filter Unit. The filtrate was purified using a Protein A column and ASEC. Fractions containing product were pooled by centrifugation (30,000 Da) and buffer-exchanged into PBS. The product was filtered through a 0.2- $\mu$ m filter under sterile conditions and frozen for storage.

## 2.3 Synthesis of ADC-2 and ADC-3

### Anti-HER2 ADC-2

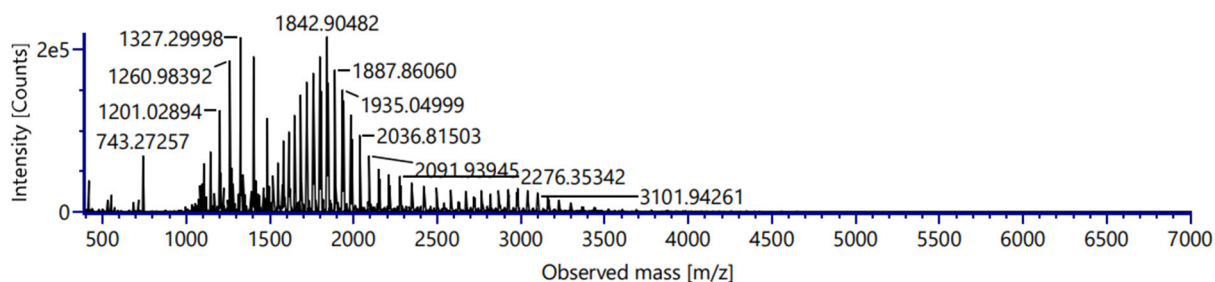
To anti-HER2 mAb (780  $\mu$ L, 3.85 mg/mL, 1 equiv.) in BBS was added TCEP-HCl (20  $\mu$ L, 10 mM in BBS, 10 equiv.) and the mixture incubated at 37 °C for 1.5 h. The reaction mixture was then cooled to 4 °C and to this was added diBrPD **Error! Reference source not found.** (80  $\mu$ L, 10 mM in DMF, 40 equiv.) and DMF (120  $\mu$ L), and the resulting mixture left to stand at 4 °C for 20 h. The excess reagents were removed *via* ultrafiltration (30,000 Da) into PBS. The conjugates were characterised by Intact MS and SDS-PAGE to determine DAR and aggregation.

### Anti-IL4 ADC-3

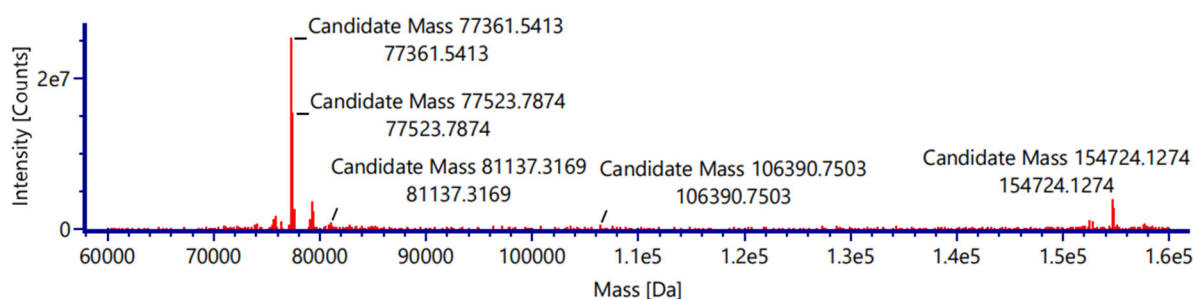
To anti-IL4 mAb (960  $\mu$ L, 3.16 mg/mL, 1 equiv.) in BBS was added diBrPD **Error! Reference source not found.** (250  $\mu$ L, 1.6 mM in DMF, 20 equiv.) and the resulting mixture left to stand at 4 °C for 2 h. After the preincubation period, TCEP-HCl (20  $\mu$ L, 10 mM in H<sub>2</sub>O, 10 equiv.) was added and the resulting mixture was left to stand at 4 °C for 20 h. The excess reagents were removed *via* ultrafiltration (30,000 Da) into PBS. The conjugates were characterised by Intact MS and SDS-PAGE to determine DAR and aggregation.

## 2.4 Mass Spectrometry of ADC-2 and ADC-3

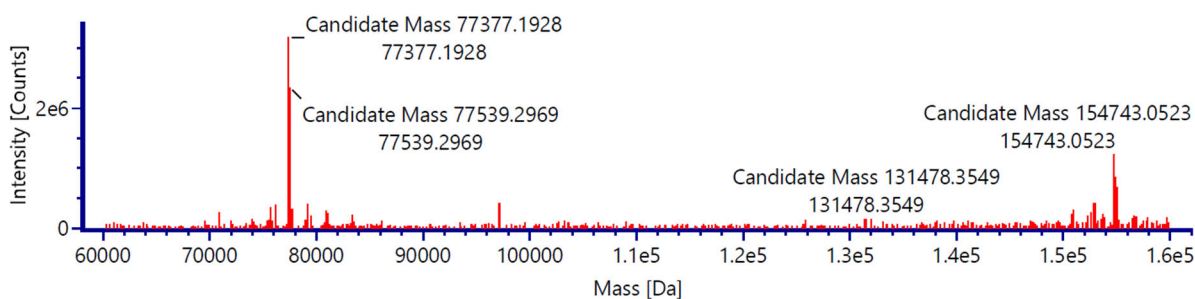
**A**



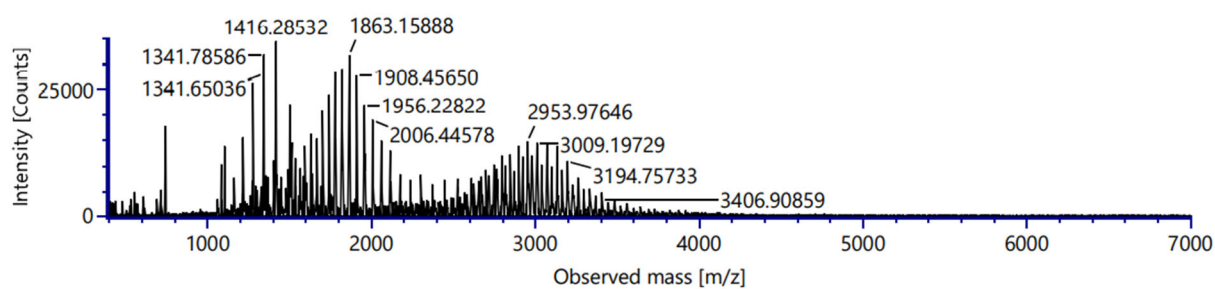
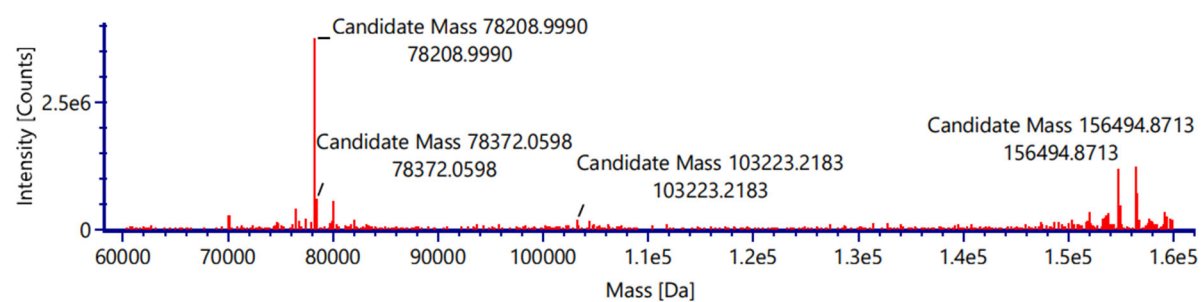
**B**



**C**



**Figure S1.** Intact MS of ADC-2: **(A)** Non-deconvoluted ion-series, **(B)** deconvoluted MS, **(C)** deconvoluted MS after 275 days stored at 4 °C.

**A****B**

**Figure S2.** Intact MS of ADC-3: **(A)** Non-deconvoluted ion-series, **(B)** deconvoluted MS.

## 2.5 SDS-PAGE of ADC-2 and ADC-3

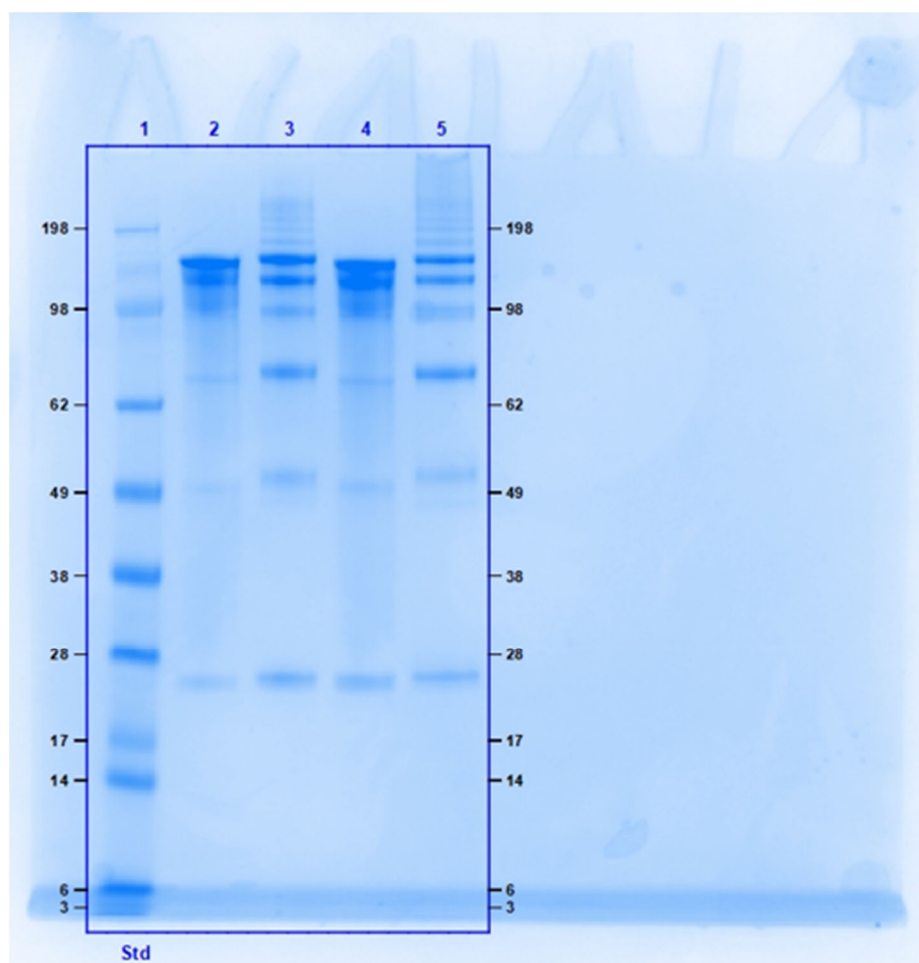


**Figure S3.** SDS-PAGE of ADC-2 and ADC-3: Lane 1 = Molecular Ladder, Lane 2 = Unmodified anti-IL4 mAb, Lane 3 = ADC-3, Lane 4 = Unmodified anti-HER2 mAb, Lane 5 = ADC-2.

## 3. Biological Assays

### 3.1 Materials and Methods

#### Cell culture

SKOV-3 warranted breast cancer cells were cultured in McCoy's 5A medium supplemented with glutamine, 10% FBS and 1% Penicillin-Streptomycin. HEK293 cells were cultured in Dulbecco's modified Eagle's medium (DMEM) supplemented with glutamax, pyruvate, 10% heat inactivated FBS and 1% Penicillin-Streptomycin. Cell lines were maintained in a humidified incubator at 37 °C and 5% CO<sub>2</sub>.

For cellular degradation, 4×10<sup>6</sup> cells were seeded in a 96-well plate, allowed to attach overnight, and incubated at 37 °C for 6 h or 16 h with the indicated compounds. Where indicated, a 1 h pre-treatment with 10 μM MG132 was performed before the addition of the compound.

#### Lysis buffer composition

The lysis buffer used consists of 10 mL RIPA buffer, 1 μL of 1 M DTT, one PhosSTOP™ phosphatase inhibitor tablet, one Pierce™ protease inhibitor tablet and 25 μL Benzonase Nuclease (Sigma Aldrich).

#### Gel electrophoresis

SDS-PAGE was carried out using Invitrogen NuPage 4-12% 1.5 mm Bis-Tris gels. Samples were mixed with loading buffer (9:1 ratio of NuPAGE LDS sample buffer 4x/NuPAGE sample reducing agent 10x) and then heated at 95 °C for 5 min. Samples were run at a constant voltage (200 V) for 60 min in Novex NuPAGE MOPS SDS running buffer (20x). The molecular ladder used was the Li-COR Chameleon Duo Pre-stained ladder.

#### Western blot analysis

After cell treatment, the media was aspirated and to each well was added 25-30 μL of lysis buffer. The cells were left on a rocker at 4 °C for 20 min before subjecting the protein extracts to SDS-PAGE. Each gel was subjected to wet transfer on low background fluorescence PVDF membranes which were then blocked with LI-COR Intercept® Blocking Buffer for 1 h at rt. The membranes were then incubated with the primary antibodies at 4 °C overnight, followed by PBS + 0.1% tween washes (3×10 min), and then incubation with the secondary antibodies for 1 h at rt (see Table S1 for antibodies). The membranes were washed with PBS + 0.1% tween (3×5 min) and then visualised using the Odyssey LCx imaging system and analysed using ImageStudio Lite Version 5.2.

**Table S1.** Primary and secondary antibodies used.

Antibody	Species	Supplier	Catalog no.	Dilution
RIPK2	Rabbit	Cell Signalling Technologies	4142S	1:1000
β-actin	Mouse	Cell Signalling Technologies	3700S	1:1000

800CW Anti-rabbit IgG	Donkey	LI-COR	926-32213	1:20000
680RD Anti-mouse IgG	Donkey	LI-COR	926-68072	1:20000

### HiBit Assay

The Promega Nano-Glo® HiBit Lytic Detection System was used for analysis according to the manufacturer's instructions. The plate was read on a PHERAstar.

### Cell viability

Cell viability was determined by CellTiter-Glo luminescent cell viability assay according to the manufacturer's instructions (Promega, G7570).

## 3.2 Uncropped blots

### SKOV3 16 h incubation

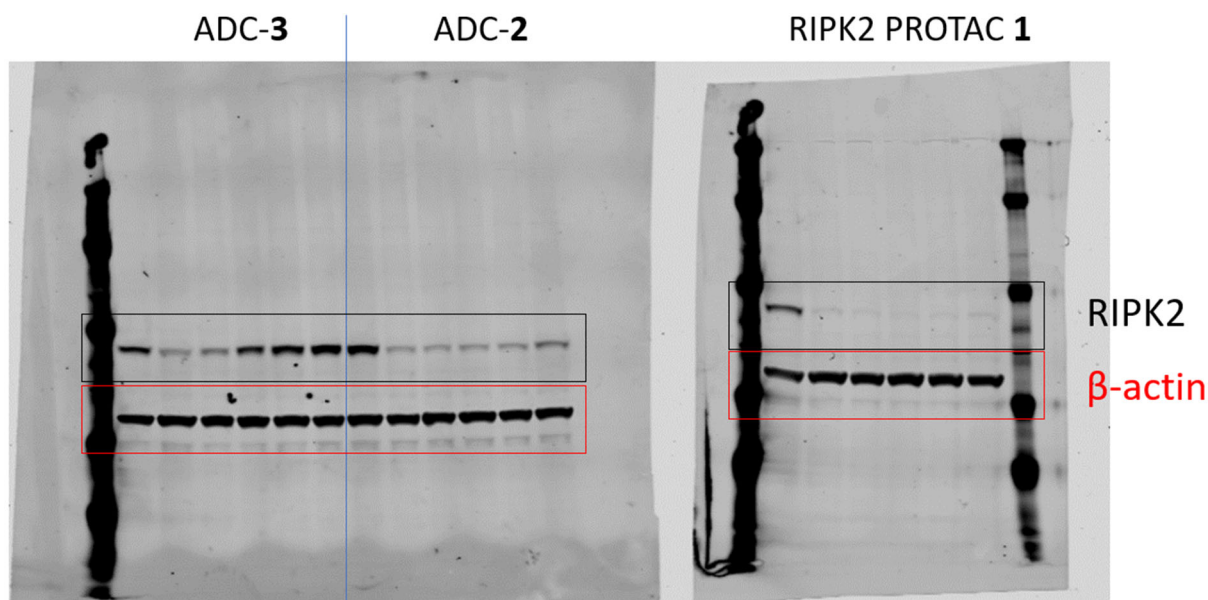


**Figure S4.** Uncropped Western blot analysis of RIPK2 degradation in SKOV3 cells following a 16 h incubation with PROTAC 1, ADC-2 or ADC-3.

SKOV3 6 h incubation

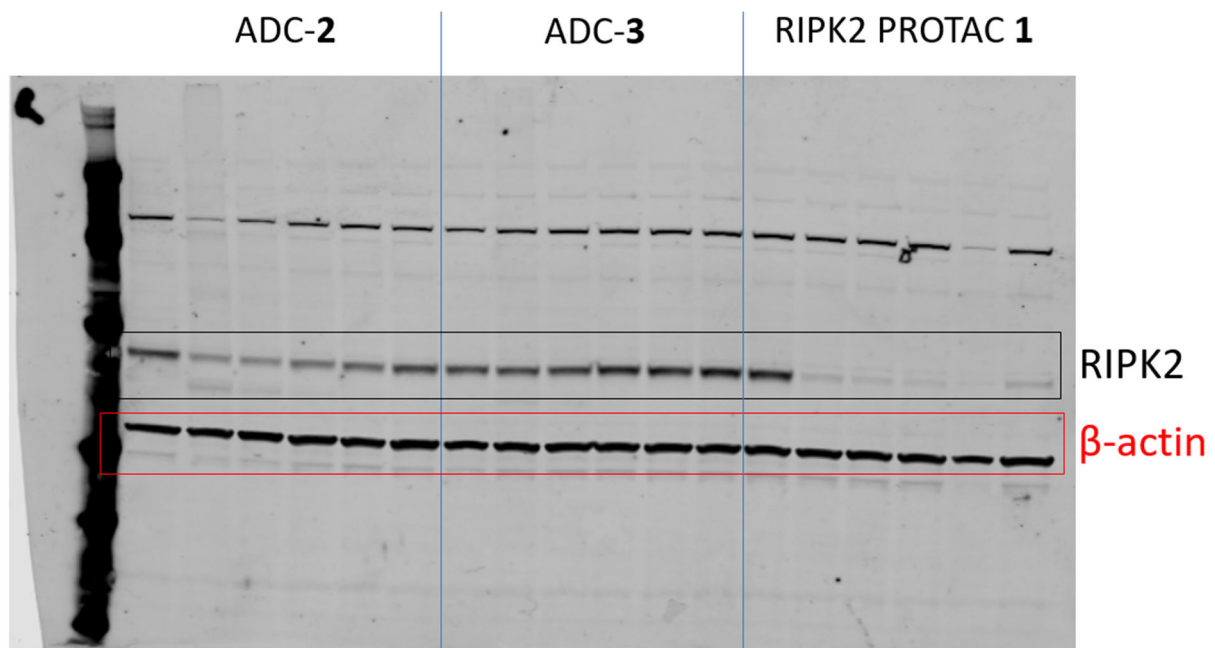


**Figure S5.** Uncropped Western blot analysis of RIPK2 degradation in SKOV3 cells following a 6 h incubation with PROTAC 1, ADC-2 or ADC-3.

SKOV3 + MG132

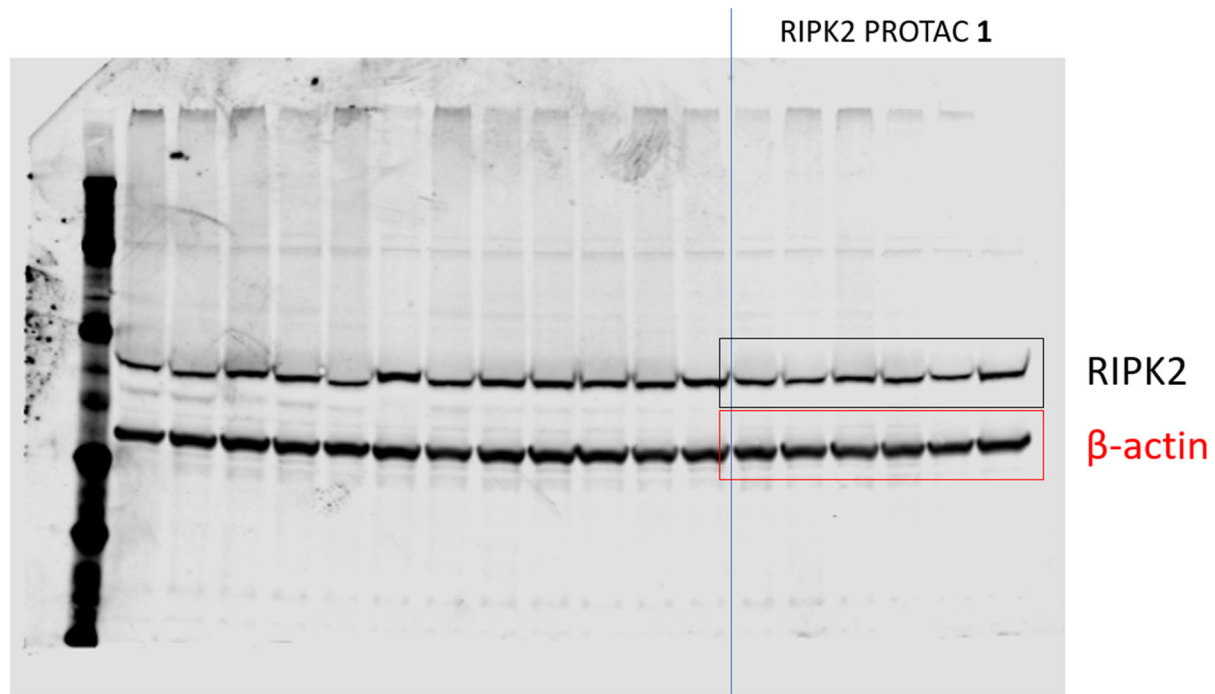


**Figure S6.** Uncropped Western blot analysis of RIPK2 degradation in SKOV3 cells following a 1 h pre-treatment with 10  $\mu$ M MG132 following a 16 h incubation with PROTAC 1.

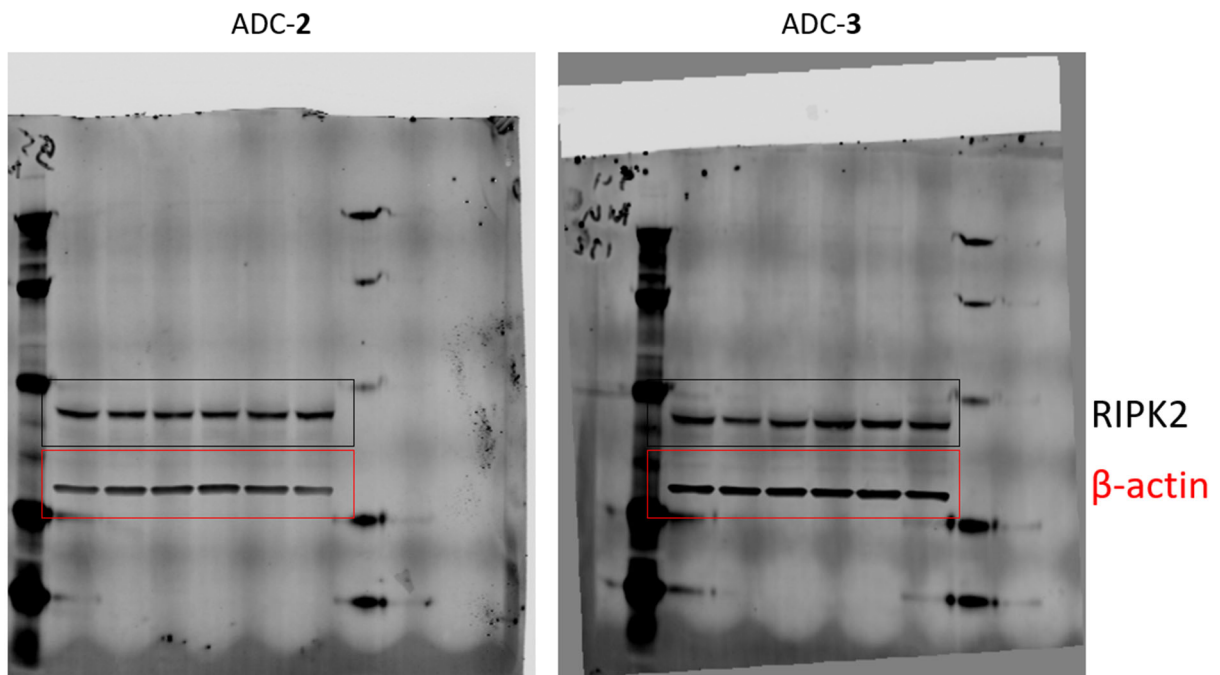


**Figure S7.** Uncropped Western blot analysis of RIPK2 degradation in SKOV3 cells following a 1 h pre-treatment with 10  $\mu$ M MG132 following a 16 h incubation with ADC-2 or ADC-3.

## 4. References

1. Bondeson, D. P.; Mares, A.; Smith, I. E.; Ko, E.; Campos, S.; Miah, A. H.; Mulholland, K. E.; Routly, N.; Buckley, D. L.; Gustafson, J. L.; Zinn, N.; Grandi, P.; Shimamura, S.; Bergamini, G.; Faeltsh-Savitski, M.; Bantscheff, M.; Cox, C.; Gordon, D. A.; Willard, R. R.; Flanagan, J. J.; Casillas, L. N.; Votta, B. J.; den Besten, W.; Famm, K.; Kruidenier, L.; Carter, P. S.; Harling, J. D.; Churcher, I.; Crews, C. M., Catalytic in vivo protein knockdown by small-molecule PROTACs. *Nat. Chem. Biol.* **2015**, *11*, 611-617.
2. Marcher, A.; Nijenhuis, M. A. D.; Gothelf, K. V., A Wireframe DNA Cube: Antibody Conjugate for Targeted Delivery of Multiple Copies of Monomethyl Auristatin E. *Angew. Chem., Int. Ed. Engl.* **2021**, *60*, 21691-21696.